Speciation of Arsenic and Selenium in Rabbit Using X-ray Absorption Spectroscopy

A Thesis Submitted to
The College of Graduate Studies and Research
In Partial Fulfillment of the Requirements
For the Degree of Master of Science
In the Department of Anatomy & Cell Biology
University of Saskatchewan, Saskatoon, Canada
By

Dongmei Liu

PERMISSION TO USE

In presenting this thesis in partial fulfillment of the requirements for a Master of Science degree from the University of Saskatchewan, I agree that the libraries of this University may make it freely available for inspection. I further agree that permission for copying of this thesis in any manner, in whole or in part, for scholarly purposes may be granted by professors who supervised my thesis work or, in their absence, by the Head of the Department or the Dean of the College in which my thesis work was done. It is also understood that any copying or publication or use of this thesis or parts thereof for financial gain shall not be allowed without my written permission. It is also understood that due recognition shall be given to me and to the University of Saskatchewan in any scholarly use which may be made of any material in my thesis.

Requests for permission to copy or to make other use of material in this thesis in whole or part should be addressed to:

Head of the Department of Anatomy and Cell Biology

University of Saskatchewan

107 Wiggins Road

Saskatoon, Saskatchewan S7N 5E5

CANADA

ABSTRACT

Chronic arsenic poisoning due to arsenic contamination of groundwater is a serious public health problem in Bangladesh and neighboring countries. Severe health effects associated with chronic exposure to arsenic include melanosis and several kinds of cancer. It is now generally agreed that the arsenic contamination of groundwater in Bangladesh is of geological origin. Arsenic naturally present in aquifers may be mobilized into drinking water by microbial action.

The formation of a novel arsenic-selenium compound: seleno-*bis* (S-glutathionyl) arsinium ion, $[(GS)_2AsSe]^-$, and its subsequent excretion in rabbit bile has been demonstrated previously. This molecular basis for the in vivo antagonism between arsenic and selenium was discovered using X-ray absorption spectroscopy. There is growing evidence that, in Bangladeshi people who are suffering long term chronic low-level arsenic poisoning, this antagonism is causing a selenium deficiency. Administering selenium supplements might provide a simple but highly effective treatment of the Bangladeshi arsenic poisoning.

In order to examine the disposition of $[(GS)_2AsSe]^-$, a set of rabbits were intravenously injected with selenite, arsenite or both. Whole blood, red blood cell and plasma samples were collected at different time intervals within 2hrs after injection and cecotrope samples 24hr after injection. Samples were examined using X-ray absorption spectroscopy and both arsenic and selenium K-near edge spectra were recorded.

Speciation of arsenic and selenium will be discussed in this thesis. Results indicate that $[(GS)_2AsSe]^-$ is formed in blood very rapidly after injection of both arsenite and selenite, and then is removed from blood stream within 2hrs post injection. Results also show that $[(GS)_2AsSe]^-$ is assembled in red blood cells, with no $[(GS)_2AsSe]^-$ detected in plasma samples. $[(GS)_2AsSe]^-$ is also found in cecotrope samples after injection of both arsenite and selenite.

The results of this study in rabbits will contribute to the understanding of chronic arsenic poisoning in humans.

ACKNOWLEDGEMENTS

First of all, I would like to express my deepest gratitude to my M.Sc. supervisor Dr. Graham George for giving me the chance to finish this project and his guidance, expertise and advice during my graduate studies. I am thankful to my committee member Dr. Ingrid Pickering, for her support, understanding and encouragement throughout my research. I would not get this far without their help and supervision.

I also would like to thank the other members of my Advisory committee: Dr. Jane Alcorn, Dr. Judith Smits, Dr. Pat Krone and Dr. Bernhard Juurlink for their valuable time and guidance at all levels of my research project.

Thanks to all the members of the Molecular and Environmental Sciences group for their time and assistance in data collection and the discussion of data analysis during my project. I am especially thankful to Michele Moroz at the Laboratory Animal Services Unit for helping with the rabbit experiments and the blood sample collection.

I also want to thank my parents. Thanks to my father Dr. Zuoxin Liu who always encourages me to face the challenge and gives my full support whenever I have difficulties. Thanks to my mother Guifang Li who takes care of me throughout the years and give me freedom to live my life. Thanks to my boy friend Eric Ren who gives me all his love and support during my thesis writing. In addition, I would like to dedicate this thesis to my grandmother who passed away last year.

I acknowledge financial contributions from Canadian Institutes of Health Research (CIHR) for supporting my studies.

Research described in this thesis was partially performed at the Canadian Light Source, which is supported by the Natural Sciences and Engineering Research Council of Canada, the National Research Council Canada, the Canadian Institutes of Health Research, the Province of Saskatchewan, Western Economic Diversification Canada, and the University of Saskatchewan. Portions of this research were carried out at the Stanford Synchrotron Radiation Lightsource, a national user facility operated by Stanford University on behalf of the U.S. Department of Energy, Office of Basic Energy Sciences.

Table of Contents

List of Tables

List of Figures

List of Abbreviations

α-Se	Elemental selenium
As	Arsenic
$As(GS)_3$	Arsenic triglutathione
AsO_3^{3-}	Arsenite
$(CH_3)_3As=O$	Trimethylarsine oxide
$CH_3As(HlipS_2)$	A sulfur correlated MMA^{III}
Cys-Se-S-Cys	Selenodiglutathione
CysSeSeCys	Selenocystine
DMA	Dimethylarsinous acid
EXAFS	Extended X-ray absorption fine structure
$[(GS)_2AsSe]^-$	Seleno-*bis* (S-glutathionyl) arsinium ion
GS-Se-GS	Selenodiglutathione
$HlipS_2^{2-}$	The reduced lipoic acid
HSe^-	Inorganic selenide

MMA	Monomethylarsonic acid
R-Se-R	Selenomethionine
Se	Selenium
SeO_4^{2-}	Selenate
SeO_3^{2-}	Selenite
SMA	S-adenosylmethionine
XAS	X-ray Absorption Spectroscopy

Chapter 1: Introduction

1.1 Selenium and Arsenic in the environment

1.1.1 Selenium

Elemental selenium has several stable allotropes: Gray selenium (polymeric Se), black selenium and the deep-red crystalline monoclinic forms, which are composed of Se_8 molecules, similar to many allotropes of sulfur (Masters, 2009 and House, 2008). Selenium is an essential trace mineral nutrient which was first discovered in 1817 (Berzelius, 1818), and it is normally found in oxidation states (Se^{2+}, Se^{4+}, Se^{6+}). It occurs naturally in several inorganic forms such as selenite, selenate and selenide. Major dietary sources of selenium include plants, meats and seafood. The levels of selenium in plants are related to the levels of selenium in soils (Thavarajah *et al*, 2007). Food animals that eat grains or plants grown in selenium-rich soil have also higher levels of muscle selenium.

Uptake of selenium depends upon the chemical form in which the element is present. Studies have shown that the absorption of inorganic forms of selenium such as sodium selenite by the gastrointestinal tract may be variable, although generally over 50%, while organic forms of selenium such as selenomethionine are almost totally absorbed (Vendeland *et al.*, 1992). Organic selenium is naturally found in two amino acids - selenomethionine and selenocysteine. Selenomethionine cannot be synthesized by

humans, but only by plants or microorganisms (Ruyle, 2009); it has no known physiological role and can be considered as a metabolic mistake in which selenium substitutes for its fellow chalgonide sulfur by dint of similar chemistry. Methionine can in principal be replaced by selenomethionine in proteins without loss of function (Whanger, 2002) and this is commonly exploited by protein crystallographers who use selenomethionine substitution to solve structures. Conversely, cysteine cannot be similarly replaced by selenocysteine due to the differing chemistries of thiolate and selenolate groups. Thus, the pKa values of selenols and thiols are typically 5 and 8, respectively, and selenols and selenolates are much more readily oxidized than the corresponding sulfur compounds.

Physiological functions of selenium include regulation of thyroid metabolism and Vitamin C redox state. Selenium is also essential for the antioxidant glutathione peroxidase enzymes. However, cancer-related possibilities have also been proposed (Russo *et al.*, 1997). A number of studies have shown that selenium is positively correlated to many beneficial health effects. Selenium helps maintain good skin, healthy eyes and eye sight, as well as improving liver function. Researchers in Finland conducted a study of serum selenium and cancer in the 1980's and showed that selenium deficiency is correlated with increased risk for certain types of cancer (Mänistö *et al.*, 2000). Other research has indicated that Vitamin E along with selenium supplement may help prevent recurrence of tuberculosis (Villamor *et al.*, 2008). Additional work has suggested that selenium could reduce the risks of developing type II diabetes (Bleys *et al.*, 2007).

Scientists have also found that there is a special link between selenium and mercury toxicity--selenium helps to remove mercury from body (Cuvin-Aralar ML and Furness RW, 1991 and Gailer, *et al.*, 2000), although epidemiological studies are inconclusive in linking selenium to protection against the adverse effects of methylmercury (Watanabe, 2002). A novel arsenic-selenium-glutathione complex has been discovered and it has been suggested that selenium supplements might prevent or cure arsenic poisoning (Gailer *et al.*, 2000). A geographical correlation between high disease rate of AIDS infection and regions of selenium deficient soils and thus low dietary selenium has been reported (Baum *et al.*, 1997), and adequate selenium intake may be correlated with reduced risk of death in HIV affected patients (Patrick, 1999).

Selenium deficiency causes Keshan Disease (Tung, 2003), which was first observed in China and in other places where selenium levels in soil are very low. Keshan Disease can cause heart muscle weakness, cardiomyopathy and higher rates of cancers, and the treatment is by dietary selenium supplementation (Chen *et al.*, 1980). The recommended amounts are fifty-five micrograms of selenium per day for healthy adult men and women, sixty micrograms a day for women during pregnancy and seventy micrograms per day for women after pregnancy (Food and nutrition board, 2000). Although individuals suffering from Keshan disease receiving selenium supplements do not show development of the disease, any damage to the heart muscle which occurred before selenium supplementation is not reversed by the treatment.

Besides Keshan disease, Kashin-Beck Disease and Myxedematous Endemic Cretinism are also related to selenium deficiency (Robert and Utiger, 1998). Kashin-Beck Disease is a degenerative osteoarticular disease involving growth and joint cartilage osteoarticular disorder that is endemic to certain areas of China, Siberia and North Korea (Moreno-Reyes *et al.*, 1998). Selenium deficiency has also been reported as a possible factor to Myxedematous Endemic Cretinism, a form of hypothyroidism which results in mental retardation (Goyens *et al.*, 1987).

Although selenium is an essential trace element, it is toxic in large doses and an excess can cause serious health problems. The maximum daily oral dose for adults is 400 micrograms. Doses exceeding 400 micrograms per day may lead to selenosis (National Institutes of Health, 2009). Symptoms of selenium toxicity include hair and tooth loss, lesions of the scalp and skin, irritability, nervous system abnormalities, brittle nails and liver and kidney problems.

1.1.2 Arsenic

Elemental arsenic is a metalloid solid which has no taste and smell. It was first discovered by Albertus Magnus in 1250 when heating realgar (As_4S_4) and soap together (Emsley and John, 2001). Arsenic is found at low concentrations everywhere in nature, approximately 5×10^{-4} of the Earth's crust, mostly in inorganic form (National Academy of Sciences, 1977). It generally occurs at low levels in rocks, soil, water, and air (Gomez-Caminero *et al.*, 2001). Depending upon environmental conditions, arsenic can exist in different valence states, as well in combination with other elements in different forms.

Under oxidizing conditions, arsenic usually exist as arsenites (As^{3+}) and arsenates (As^{5+}). These compounds in the human body can be methylated to form monomethylarsonic acid (MMA) and dimethylarsinic acid (DMA) (Huerga *et al.*, 2004). In mineralogy, arsenic is mostly found bound to sulfur, such as orpiment (As_2S_3), realgar (As_4S_4) and arseno-pyrite (FeAsS).

Arsenic and many of its compounds are potentially toxic. The health effects of arsenic are different for different chemical forms. In general, inorganic arsenic compounds with hard ligands are more toxic than organic arsenic compounds, and trivalent form of arsenic is more toxic than pentavalent and elemental forms (Styblo *et al*., 2000). In addition, certain organic arsenic compounds, such as arsenobetaine found in marine animals, are non-toxic. Arsenic is widely distributed in nature, thus low levels of arsenic may be found in a wide range of foods. Fish, seafood, cereals, wine, and cereal products are the main dietary source of arsenic. Both organic and inorganic forms of arsenic can be found in foods. Although the contents of each are related to the type of food, inorganic arsenic is rarely found at high levels.

Trivalent arsenic is known for its affinity for sulfur, and this is the bioinorganic basis of its lethality at high doses. As(III) species such as arsenite kill by respiratory poisoning by binding to the essential di-thiol of lipoic acid in enzymes such as pyruvate dehydrogenase, the terminal enzyme in glycolysis (Schiller *et al.*, 1977). This is also the biochemical basis for the lethal effects of arsenic-based war gases such as Lewisite, which is primarily chlorovinyl arsine dichloride. Other trivalent arsenicals such as the

mono-functional Adamsite (diphenylaminechlorarsine) are less lethal and have been used as riot control agents in the USA, although their mechanism of action is unclear. The pentavalent arsenates are toxic too, and also attack the pathways of glycolysis, but instead of blocking the pathway by enzyme inhibition they can act as phosphate analogues causing uncoupling of oxidative phosphorylation (Crane and Lipman, 1952).

At sub lethal doses that are less than immediately fatal the metabolism of arsenic is important in determining its physiological effects. Many mammalian species can methylate inorganic arsenic, but not all. (Vahter, 1994). Variable rates and extent of methylation of inorganic arsenic may occur between different species (Hughes, 2002). The generally accepted methylation pathway of arsenic is shown in Figure 1.1 (Aposhian and Aposhian, 2006). The most possible mechanism is that inorganic arsenic is reduced from As(V) to As(III), followed by oxidative methylation to As(V) organic arsenic (Thomas *et al.*, 2001). The metabolism of arsenic in liver involves methylation with or without enzymes (Vigo and Ellzey, 2006), and is affected by body glutathione, methionine levels and choline status (Roy and Saha, 2002). Methylation occurs through methyltransferase enzymes involving S-adenosylmethionine (SAM) as a source of the methylation. The resulting metabolites monomethylarsonic acid (MMA^{III}) and dimethylarsinous acid (DMA^{III}) are excreted in urine (Aposhian *et al*., 2000).

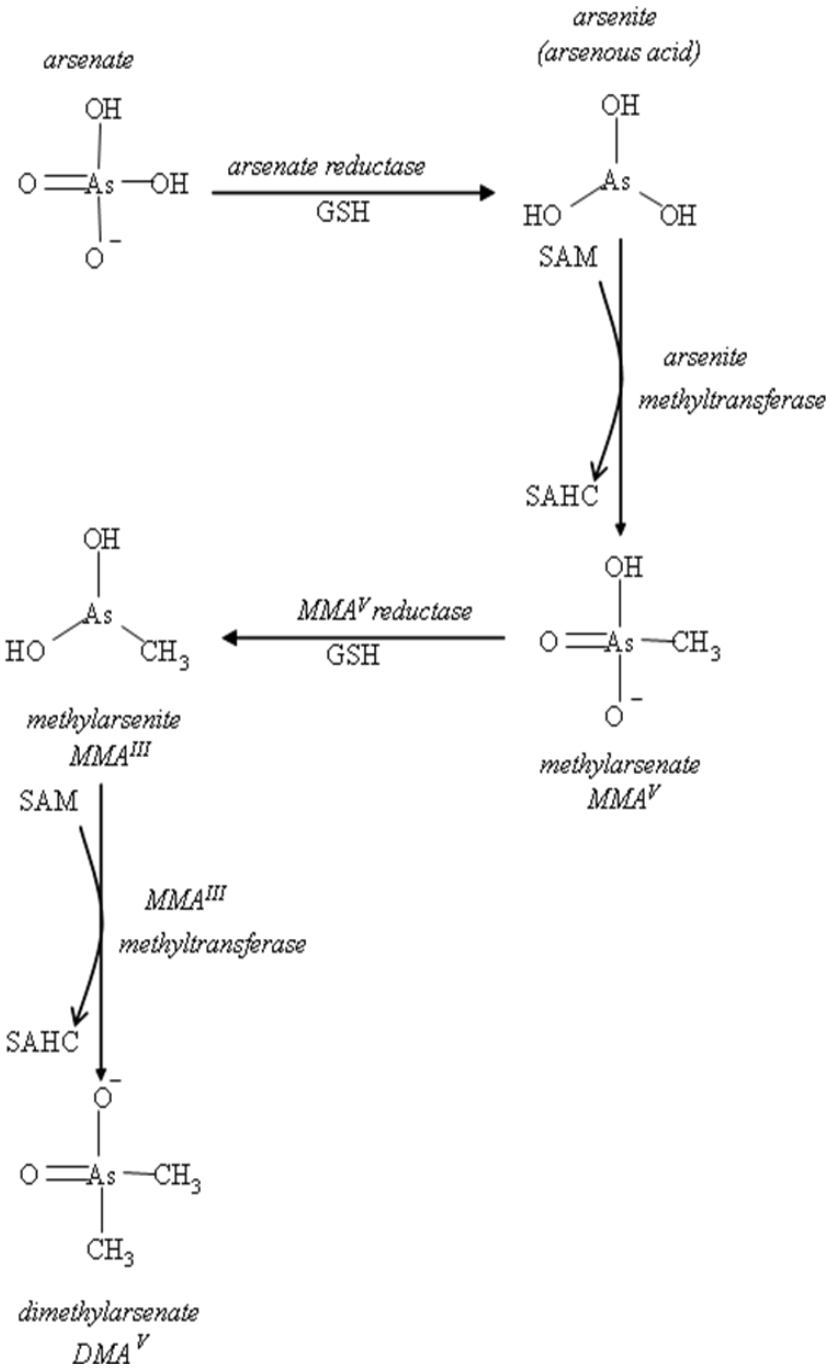

Figure 1.1 Generally accepted methylation pathway of inorganic arsenic. Modified from "Arsenic Toxicology: Five Questions", (Aposhian and Aposhian, 2006).

Researchers started to believe that arsenic can have a role in inducing cancers in 1987 (Hutchinson, 1987). Arsenic has been correlated to different types of cancers, like skin cancer, liver cancer, kidney cancer and lung cancer (NTP, 2000). Although there is still debate about possible mechanisms of cancer causation, it is widely believed that DNA repair inhibition and/or alterations in the status of DNA methylation are involved. Increased frequency of sister-chromatid exchanges, micronucleus (Warner *et al.*, 1994 and Gonsebatt *et al.*, 1997) and chromosomal aberrations are correlated with increased arsenic exposure (Mäki-Paakkanen *et al.*, 1998).

Arsenic is very well known for its poisonous nature at high doses. Its use during Victorian times as a homicidal agent gave rise to the term "inheritance powders" which were usually arsenic trioxide (As_2O_3). Despite this infamy there are medical applications of the element, some of them are quite valid. During the 20th century, several arsenic compounds have been used as pharmaceuticals, for example, arsphenamine is used to treat syphilis, Fowler's solution is used to treat skin diseases, and Pearson's Arsenical Solution is used for parasitic infestation (Breslow and Cengage, 2002). In 2000, the US Food and Drug Administration approved arsenic trioxide (As_2O_3) – the same compound which was the active ingredient in Victorian "inheritance powders" and also known by the trade name Trisenox®, for the treatment of patients with acute promyelocytic leukemia (Antman, 2001). Arsenic compounds are also used in pigments, wood preservation, insecticides, copper and lead alloys, glass and poison gases (e.g., Lewisite) as a chemical weapon (Rahman *et al*., 2004).

1.2 Arsenicosis

Human exposure to arsenic includes occupational exposure and the ingestion of contaminated drinking water and seafood. Arsenic absorbed by inhalation and orally, can also be excreted in urine. In some areas, arsenic exposure in drinking water is a considerable source of daily inorganic arsenic intake (Gomez-Caminero *et al*., 2001).

Arsenicosis—chronic arsenic poisoning due to arsenic contamination of groundwater—has been recently noted as a serious public health problem in Bangladesh (Chaudhuri, 2004) and neighboring countries. Reports have shown that approximately 57 million people are drinking groundwater with arsenic concentrations greater than the World Health Organization's standard of 10 µg/L (Petrusevski *et al*., 2005). The daily intake of total arsenic from food and beverages is generally between 20 and 300 µg/day (Steiner-Asiedu *et al.*, 2010). The acute lethal dose of arsenic to human beings has been estimated to be 0.6 mg/kg/day (Dart, 2004).

Severe health effects associated with chronic exposure to arsenic include melanosis, symmetric hyperkeratosis of palms and soles, depigmentation, Bowen's disease, basal cell carcinoma, diabetes, bladder cancer, liver disease and birth defects (Robson *et al.*, 1963). Residuary arsenic in nails and hair can be detected even years after the exposure. In Bangladesh today, there are between 30 to 80 million people who get their drinking water from the tube-wells that were installed for the prevention of diarrhea originally. These wells were built years ago by international aid agencies to help reduce water-borne diseases and give local people a clear source of water instead of using the dirty, disease

infested ground water. It is estimated about 130 million people which is 90% of the population in Bangladesh prefer to drink well water (WHO, 2001). Only a bit greater than 10% of the Bangladeshi people who live in the large agglomerations and some district towns have access to the piped water supplies (WHO, 2001).

It is now generally accepted that geological origin causes the groundwater in Bangladesh being contaminated by arsenic. Scientists found that the well drilled in Bangladesh with the highest arsenic concentration has been there for many years, when arsenic has been released from the sediments and infiltrated to underground from the surface after microbial metabolism. Arsenic present in drinking water in Bangladesh is mainly As(III) with lower levels of As(V), with a ratio of 9:1 (Spallholz *et al*,. 2006). Scientists have adopted several physical-chemical treatment methods to remove arsenic from drinking water, such as adsorption-co-precipitation using iron and aluminum salts and ion exchange (Mortoza, 1997). But these treatments are neither applicable to a mass of tube wells nor highly effective. Chelation therapy may help relieve some of the symptoms and improve clinical manifestations. However, the damage in several organs due to chronic arsenicosis is irreversible and there is no effective therapy for these diseases (Guha Mazumder, 2008). It is obvious that scientists and researchers should find an important and effective method to prevent and treat arsenicosis.

1.3 Antagonism between Arsenic and Selenium

Arsenic and Selenium have similar chemical properties, but their biological effects are very different (Zeng *et al*., 2005). Therefore, the interaction between arsenic and selenium depends on their different chemical forms. In general, arsenite and selenite are the most common oxy-ion of arsenic and selenium in the environment, respectively. When arsenite and selenite are administered separately, they are toxic, but when these two compounds are given together, the toxicity is cancelled. The antagonism between arsenic and selenium was first discovered in the 1930's (Moxon, 1938). Evidence has shown that arsenic compounds can protect against a variety of different forms of selenium (Levander, 1977). It is reported that sodium arsenite, can not only active against sodium selenite, but also selenocystine (Du Bios *et al.*, 1940). Experimental results have also suggested that arsenite can fight the toxicity of selenite in different animal species (e.g. dog, swine, and cattle) (Levander, 1977). Although the antagonism between arsenic and selenium has been reported since 1938, the mechanism still remains unclear.

In 2000, the molecular basis of the *in vivo* antagonism between arsenite and selenite was discovered. The formation of a novel arsenic-selenium compound: seleno-*bis* (S-glutathionyl) arsinium ion, $[(GS)_2AsSe]^-$ (Figure 1.2), which is subsequently excreted in rabbit bile was demonstrated (Gailer *et al.*, 2000). The details of the arsenic-selenium-glutathione complex were elucidated using X-ray absorption spectroscopy.

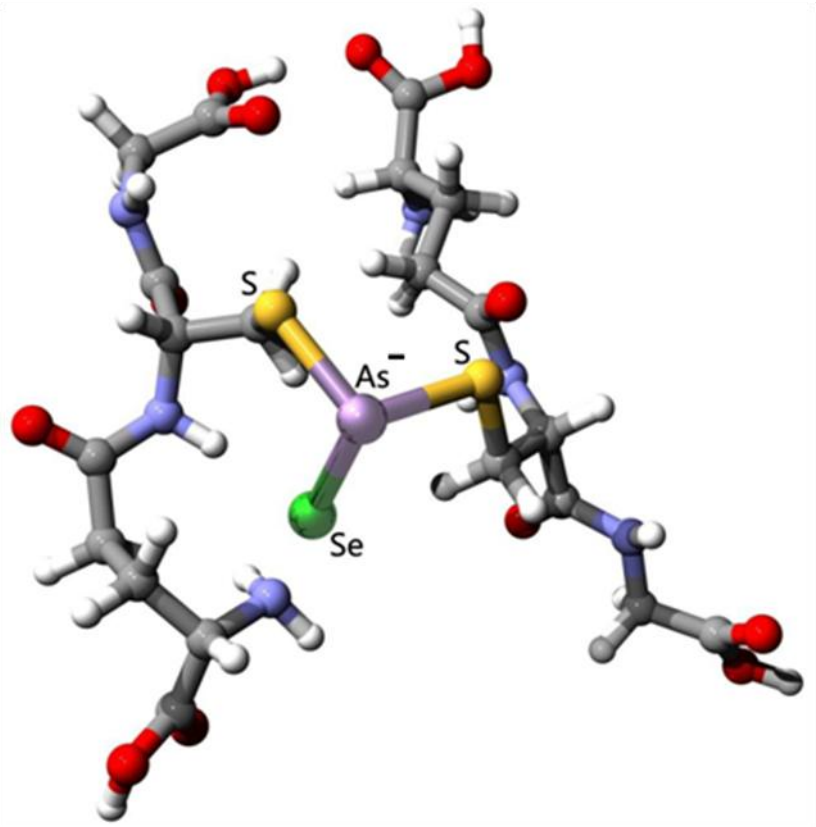

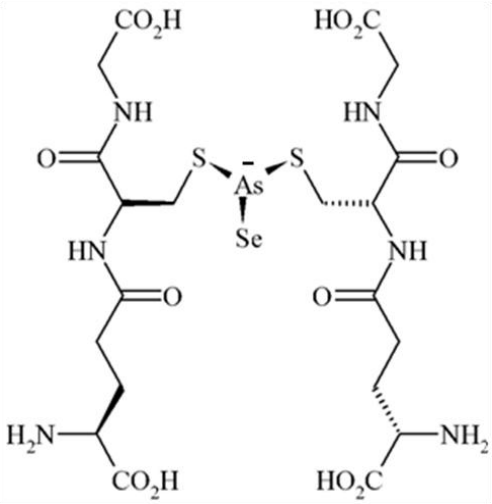

Figure 1.2: Structure of the seleno-bis (S-glutathionyl) arsinium ion, which is abbreviated $[(GS)_2AsSe]^-$.

In earlier work, a New Zealand white rabbit was used as animal model to determine the molecular basis of the antagonism of arsenite and selenite. After the simultaneous administration of environmentally relevant doses of arsenite and selenite, $[(GS)_2AsSe]^-$ was excreted from the bile of the rabbit (Gailer *et al.*, 2004). This evidence suggests that the *in vivo* formation of this metabolite comprises an important mechanism of toxicology. The chemical reaction of this mechanism has been predicted as the following chemical equation:

$$As(OH)_3 + HSeO_3^- + 8GSH \rightarrow [(GS)_2AsSe]^- + 3GSSG + 6H_2O \quad [1]$$

According to equation [1], 1 mole of arsenite and 1 mole of selenite with 8 mole equivalents of glutathione forms $[(GS)_2AsSe]^-$ (Gailer *et al.*, 2000). Consequently, it is important to have high concentrations of glutathione to form $[(GS)_2AsSe]^-$ from arsenite and selenite *in vivo* of mammals.

1.4 Hypothesis and Objectives

1.4.1 Hypothesis

Because biliary excretion of $[(GS)_2AsSe]^-$ would unavoidably consume the body load of selenium then insufficient dietary intake of selenium might cause of selenium deficiency. Furthermore, the symptoms of selenium deficiency are very similar to those of Bangladeshi people who are suffering long term chronic low-level arsenic poisoning. Accordingly, our research group has hypothesized that those patients who experienced arsenicosis in Bangladesh are in fact suffering a selenium deficiency. We propose the following experiments to further understand the formation and elimination of $[(GS)_2AsSe]^-$, and to build a scientific basis for treatment of arsenicosis. The hypothesis to be tested in the work presented in this thesis is that the *in vivo* chemistry of arsenic and selenium can be monitored using X-ray absorption spectroscopy of blood samples, and that this can be used to develop an understanding of the formation and elimination of $[(GS)_2AsSe]^-$. Using rabbit as our animal model, we expect that the speciation results of arsenic in blood will be different when administering arsenite alone or with selenite simultaneously. We propose that $[(GS)_2AsSe]^-$ can be detected in blood samples very rapidly after injection of arsenite and selenite, and will be eliminated from blood stream after a certain period of time post injection. In addition, $[(GS)_2AsSe]^-$ might be found in cecotrope samples after injection of both arsenite and selenite. The experiments proposed in this thesis will also lead us to the answer of whether $[(GS)_2AsSe]^-$ is assembled in red blood cells or plasma *in vivo*.

1.4.2 Objectives

Experiments described in this thesis are trying to answer the following questions:

1. How fast does $[(GS)_2AsSe]^-$ form?

Rabbits will be injected either with arsenite, selenite or both, and samples of whole blood will be taken at a series of times. Both As and Se K-edge spectra will be recorded, and this will give information on how fast $[(GS)_2AsSe]^-$ forms.

2. How fast is $[(GS)_2AsSe]^-$excreted?

Blood samples will also be collected at chosen times and As and Se K-edge spectra will be recorded to see how fast $[(GS)_2AsSe]^-$ is eliminated from blood.

3. What is the speciation of arsenic and selenium in blood and cecotrope?

Blood and cecotrope samples will be also collected at chosen times and As and Se K-edge spectra will be recorded to analyze the speciation of arsenic and selenium.

Chapter2: Experimental Technique

2.1 X-Ray Absorption Spectroscopy

X-ray Absorption Spectroscopy (XAS) is an experimental technique which can be widely used to determine the physical and electronic structure of matter. XAS is element specific and can provide chemical speciation information of metals and metalloids (Schulze and Bertsch, 1995). X-rays have a wide range of wavelengths, and these highly energetic photons are used to measure the molecular structure of samples. One of the main methods of analyzing the atomic level of new materials is X-ray crystallography. However, in order to use this method, the new material must be crystallized first. But no pre-treatment of digestion, drying or extraction is required for XAS to test metal or metalloid materials (George *et al.*, 2007). XAS can also yield limited molecular structural information of amorphous samples and it can probe solid, liquid, gas or even mixture samples.

A typical X-ray absorption spectrum at the selenium K-edge is shown in Figure 2.1. XAS is divided into different regions—pre-edge, near-edge and extended X-ray absorption fine structure (EXAFS). The region before the edge rise is called the pre-edge region, where the X-rays have insufficient energy to eject a core-electron. At a well-defined X-ray photon energy, a sharp rise in absorption coefficient is observed which corresponds to the transition of the core electrons to continuum. The X-ray absorption near-edge structure is extended in the first 30-40eV past the absorption edge where X-ray

photons has just enough energy to eject a core-electron. Near-edge features can provide important information of electronic structure and near-edge spectra are sensitive to oxidation state, nature of ligands and coordination geometry (Van Elp *et al*., 1995). Near edge spectra of each forms of an element is often highly distinct, and can therefore be used to identify unknown chemical species by a simple comparison with spectra of known standard compounds. There is an increasingly use of near-edge spectra to analysis chemical speciation in complex and mixtures, such as sediments, soil and organisms in environmental sciences as well as tissue samples in life and health sciences (George, 2010).

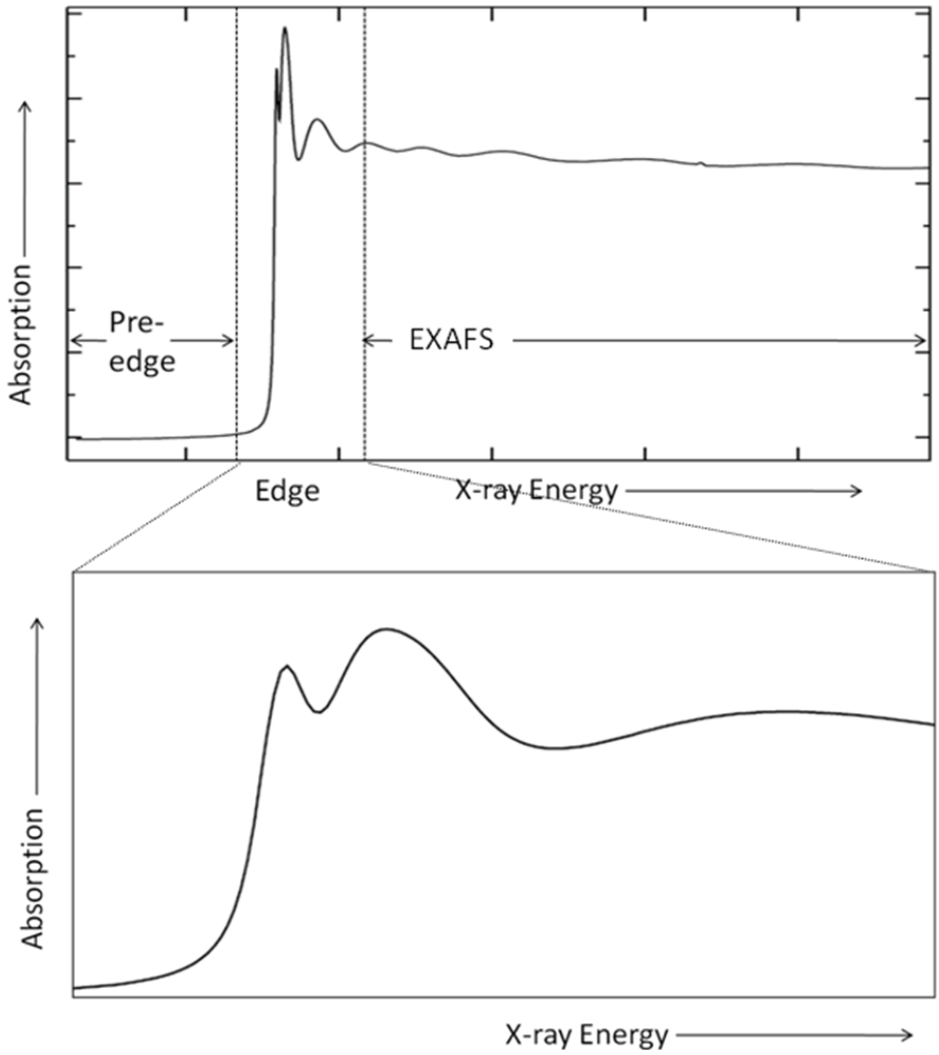

Figure 2.1 A typical XAS spectrum of a Selenium K-edge.

Upper figure shows the full spectrum of the pre-edge, edge, and extended X-ray absorption fine structure (EXAFS) regions. Lower figure shows an expanded view of the near edge region.

EXAFS was observed early in the 20'th century by Kronig. The exact origin of the structure was unclear until the 1970's when Sayers, Stern and Lytle were finally able to explain the nature of EXAFS and proved how EXAFS can be used as quantitative structural probe (Sayers *et al.*, 1979). Understanding the origins of the EXAFS allows estimation of the distance between absorber atom and backscatterer atom, as well as approximation of numbers of electrons around backscatterer since more electrons provide more effective backscatterer. From EXAFS, it is possible to determine the number of a particular type of backscatterer at a particular distance.

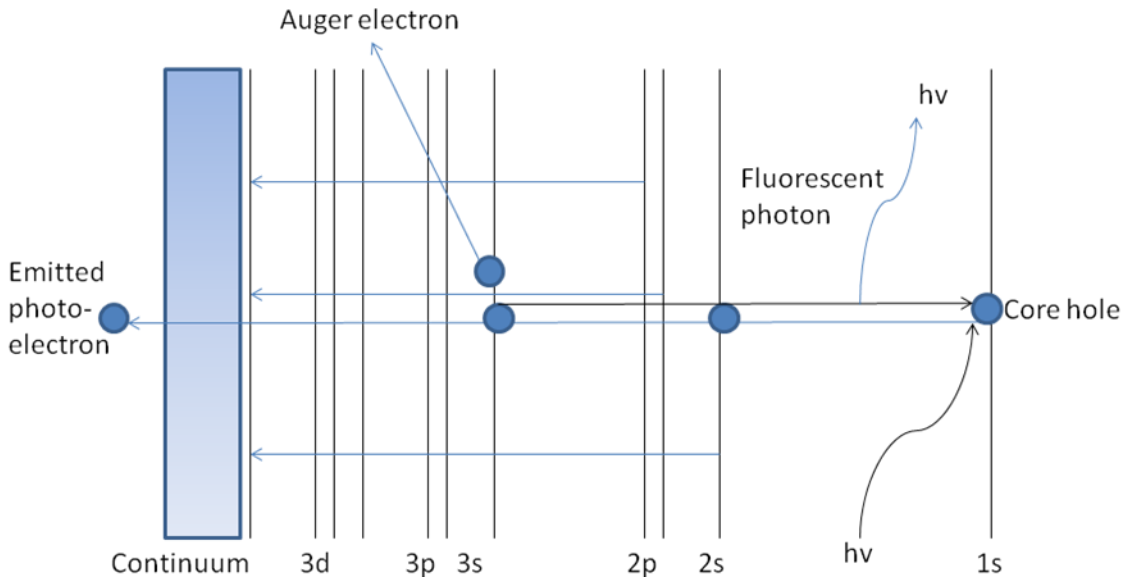

Figure 2.2 Schematic illustrations of the fluorescence radiation and Auger electron emission concomitant with X-ray absorption.

X-ray absorption occurs due to core electrons absorbing the X-ray and being ejected from the atom as photoelectrons. As shown in Figure 2.2, the absorption of an X-ray photon creates a core hole, which can be filled by decay of an out electron via different mechanisms.

First, the core hole could be filled concomitantly with X-ray fluorescence emission. This occurs when the outer electron releases its extra energy by emitting X-ray fluorescence while it decays from an outer line to fill the core hole. The energy difference between the outer and inner electrons is the same as the fluorescence photon energy. Absorption by different core levels gives rise to different X-ray absorption edges. For example, at lower energies, ejection of 3d electrons gives rise to the $M_{V,IV}$ absorption edges. At higher X-ray energies, ejection of 1s electrons gives rise to the K absorption edge.

The core hole created by X-ray absorption may be filled by the decay of an outer electron, with a concomitant emission of an Auger electron (George *et al.*, 2007). The kinetic energy of the Auger electron is the energy difference between the initial and final state of the atom (Teo *et al.*, 1986).

2.2 Synchrotron Radiation

A tunable X-ray source is required to generate X-rays and measure the energy-dependent absorption coefficient of a material. A synchrotron light source generates a high-intensity, tunable source of X-rays. An electron gun fires bunches of electrons through tubes into the booster ring (CLS, 2010). Microwave energy is then used to accelerate the electrons up to nearly the speed of light (Elder *et al.,* 1947). The electron beam is then ejected into synchrotron storage ring, where these high-speed high-energy electrons are bent by magnets inside the storage ring, or by the insertion devices such as wigglers and undulators. Wigglers and undulators are insertion devices in a synchrotron where the electron beam would normally go straight. A wiggler is the high-field case while an undulator is the low-field case.

In general, different optical elements are used in a synchrotron to generate a beam which has a broad distribution both in energy and space. In synchrotron facilities, a beamline is the instrumentation that carries beams of synchrotron radiation to an experimental end station. Figure 2.3, (A) shows a plan view of components for a modern X-ray beamline for XAS. At the front end are the X-ray optics, and the experimental station is at the end. The front end houses wiggler, safety value and photon shutters. X-ray optical component includes collimation mirror, monochromator and focusing toroid.

A monochromator is the principal optical device that we use to select a narrow band of wavelengths of light from a wider range of energies. A double crystal monochromator allows the diffracting beam to be parallel with the incident beam.

Monochromator crystal material must have excellent stability to X-rays, thermal loading, crystal perfection and narrow rocking curve (Kudo, 1965). Silicon is the most widely used material. In a typical XAS beamline, the first mirror collimates the beam through monochromator and the second mirror is used to focus the beam horizontally and vertically on the sample. Both mirrors can be used for harmonic rejection by choosing mirror material and tilt angle so that fundamental energy is reflected, and harmonic energy is absorbed.

Figure 2.3 (B) shows a plan view of a typical XAS experimental setup. A liquid helium cryostat is used to cool the sample to reduce radiation damage and make EXAFS more intense because of freezing out of atomic vibrations (George *et al*., 2007). A fluorescence detector is used to detect the fluorescence accompanying the X-ray absorption process. Typically a solid state germanium array detector or a fluorescent ion chamber detector is used, depending on the different concentration ranges. The sample is set at 45 degree to the beam and the fluorescence detector is set at 90 degree to the beam and 45 degree faces to the sample plane. This will help to reduce the intervention of Compton scattering. A standard foil of the element of interest is used for energy calibration.

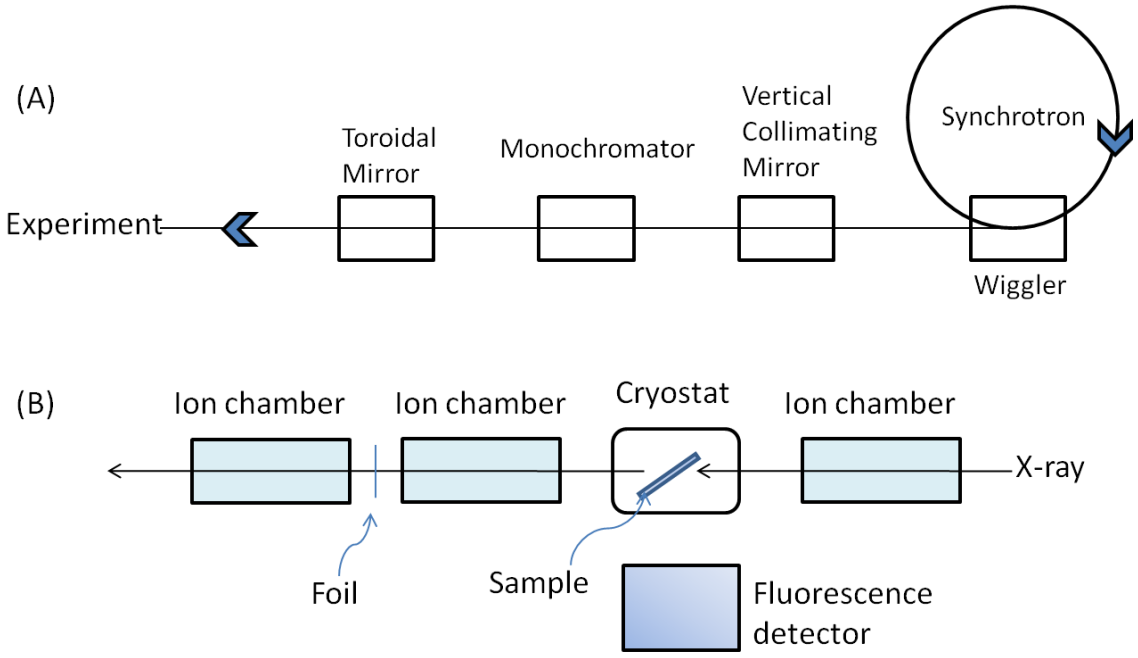

Figure 2.3 (A) Schematic optical component layout of a typical X-ray beamline for XAS (B) Plan view of a typical XAS fluorescence experiment setup

Chapter 3: Materials and Methods

3.1 Animal Model and treatment

3.1.1 Animal Model

Rabbits were chosen as an animal model in preference to rat and mouse because rabbit hemoglobin is a better model of human hemoglobin. In particular, rat and mouse hemoglobin includes cysteine residues which can interact with arsenic species (Lu *et al.*, 2004; Petric *et al.*, 2000; Carter *et al.*, 2003). These thiols are not present in either rabbit or human. Thus, arsenic binding to rat hemoglobin can be 3-16 fold greater than human hemoglobin (Aposhian, 2006), and consequently rat does not provide a good model for arsenic metabolic research. Instead, rabbit and hamster turn out to be more reasonable models (Aposhian, 2006). In order to facilitate collection of blood samples, rabbits were chosen as the animal model in our experiments.

Male New Zealand white rabbits (1.5-2kg) were purchased from Charles River Laboratories International (Wilmington, MA, USA) and maintained for 1 week before experiments on a “high fiber” rabbit diet at the Laboratory Animal Services Unit, College of Medicine, in University of Saskatchewan. Each rabbit was kept in separate cage and was taken care of by animal care professionals. All animal studies conduct in this thesis received approval from the institutional animal research ethics board for the experimental use of the rabbits.

3.1.2 Treatment

For each rabbit studied, vein catheters were placed. Rabbits were placed in a cat bag, and the hair over the artery was removed by shaving with a straight razor blade. An IV extension set was flushed with sterile saline and the syringe was left on the end of the extension set. Oil of wintergreen was applied with the cotton-tipped applicator to the skin over the artery to dilate the vein, and a 22 G catheter was then inserted into the vein. The IV extension set was then attached to the catheter which was flushed with 0.5 ml Saline, the IV extension was then locked and the saline syringe removed. The catheter was then glued to the ear with tissue glue and the extension set secured to the ear with surgical adhesive tape.

Following preparation of the rabbits the test compounds were injected. Arsenite (0.30 mg As/kg of body weight) or selenite (0.32 mg Se/kg of body weight) were dissolved in 20mM PBS (phosphate buffered saline) and adjusted to pH=7.4. Depending on the body weight of each rabbit, 1.5-2ml 0.30mg/ml arsenite or 0.32mg/ml selenite solution were injected to the rabbit, and when administering both chemicals, there was a 3-min interval in between doses. The dose of arsenite or selenite was chosen so as to be approximately one quarter of the LD_{50} for rabbit. Four rabbits were investigated using different treatments. The first was given selenite solution only (dose as above). The second rabbit was given arsenite solution only (dose as above). The third rabbit was treated with arsenite first and then 3min later followed with selenite solution. The fourth rabbit was treated with selenite first and then followed with arsenite 3min later.

3.2 Sample Preparation

3.2.1 Blood Sampling

3ml of whole blood samples were collected and mixed with heparin from each animal via the auricular vein catheter at the following time intervals post injection (after second dose when both were injected): 5 min, 20 min, 40 min, 60min, 2hr, 4hr and 24hr. Rabbits were conscious during all procedures. Blood samples before injection of test compounds were also collected as a control. Plasma and red blood cell samples were centrifuged and separated from whole blood samples collected at each time interval. At each time point, sample was immediately placed in 2mm sample cells (Figure 3.1) and frozen in liquid nitrogen for XAS analysis. Liquid nitrogen exists as liquid between 63K and 77.2K (-346 ℉ and -320.44 ℉), samples kept in Dewars filled with liquid nitrogen were stable.

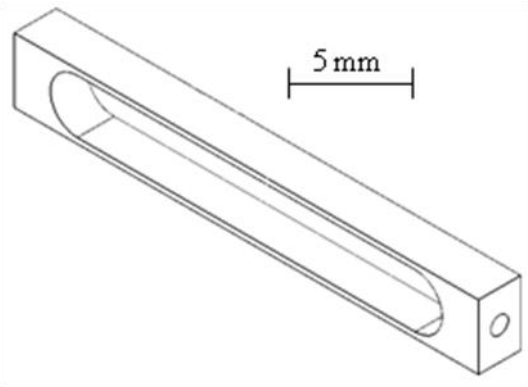

Figure 3.1 A typical 2mm pin-hole XAS sample cell.

3.2.2 Cecotrope Sample Preparation

Cecotrope are produced at night and ingested by the rabbit and so re-enter the gastrointenstinal tract. Rabbits eat cecotropes to get essential nutrients (Hirofumi, 2001). In order to stop rabbits from eating their cecotropes, a collar was put around the neck of the rabbit after injection of test compounds. After injection of 24hrs, cecotrope samples were collected and collar was removed from the rabbit. Cecotrope samples were ground and packed in 2mm sample cells and immediately frozen in liquid nitrogen for XAS analysis.

After collecting all the blood and cecotrope samples, rabbits were euthanized by injection of Phenobarbital.

3.3 Data Collection and analysis

3.3.1 Data Collection

All data present in this thesis were collected at Canadian Light Source (CLS) on the hard X-ray Micro-Analysis (HXMA) beamline as well as on Structural Molecular Bio-XAS beamlines 7-3 and 9-3 at Stanford Synchrotron Radiation Laboratory (SSRL). CLS is a third-generation synchrotron facility with a 2.9GeV storage ring and a 250mA ring current. SSRL has a SPEAR storage ring containing 250mA at 3.0GeV. At all beamlines, samples are maintained approximately at 10K in a liquid helium flow cryostat. The Arsenic and Selenium K-edge spectra are recorded. At both HXMA and 9-3 beamlines, there are an upstream collimating mirror, a Si (220) double-crystal monochromator and a downstream focusing mirror. The incident X-ray intensity is monitored using N_2 filled ionization chamber. Near-edge spectra are recorded by monitoring the K_α fluorescence using a 30-element germanium detector.

The energy is calibrated with reference to the lowest energy inflection point of the elemental foil (α-arsenic or hexagonal selenium), which are assumed to be 11867.0eV and 12658.0eV.

3.3.2 Data Analysis

Background subtraction, normalization and edge fitting were carried out according to standard methods using the EXAFSPAK program in this thesis. EXAFSPAK is a suite

of computer programs for analysis of X-ray Absorption Spectra written by Dr. Graham George and Dr. Ingrid Pickering (George *et al.*, 2000).

The raw data file contains all channels of the detector from one single scan. Before analyzing data, every scan of data should be investigated by eye for quality and consistency. Individual sweep can be excluded if there are any bad channels. The spectrum of a mixture of more than one chemical form of an element appears as the sum of the spectra of the individual components. The height of the edge jump of each component is proportional to the quantity of the element in that form. The spectrum is normalized so that the edge jump is unity. With normalized spectra, the height of the edge jump of each component is proportional to the fraction of the element present in that form. Near edge fitting are carried out by Least-square DATFIT program in EXAFSPAK.

In DATFIT program, a library file is created which contains the spectra of the standard compounds that were selected to be used in the fit. Data were then compared with the standard compounds. In Least-square fitting, equation (1) and (2) are used to calculate the fraction of each component. The program of DATFIT gives us e.s.d., residual, total and the plotting after the fit. E.s.d. means the estimated standard deviation derived from the diagonal elements of variance-covariance matrix (George *et al*., 2000). In general, three times of the e.s.d. is quoted, which stands for the 99% confidence limit. The average sum of squares of the differences between calculated and observed normalized intensities is residual. As a given unknown spectrum, the smaller the residual the better the fit is. Total is the sum of the fractions of each component, which ideally should add up to one. From eye inspection of the plotting of the residual, noise or

substantial features can be depleted. Also, thought must be given to determine if the components from the fitting are chemically reasonable for the sample. Once e.s.d, residual and chemical seems reasonable, the results can be finalized. All standard spectra of selenium and arsenic compounds in this thesis were collected at CLS on beamline HXMA and beamline 9-3 at SSRL.

$$F = \frac{1}{N}\sum_{j=1}^{N}\left(y_{j,obs} - y_{j,calc}\right)^2 \qquad \text{Equation (1)}$$

$$y_{j,calc} = \sum_{i=1}^{m} x_i I_{i,j} \qquad \text{Equation (2)}$$

$\boldsymbol{F}$ – Function being minimized by non-linear regression

$\boldsymbol{y_{j,obs}}$ – Observed intensity of mixture spectrum at energy j

$\boldsymbol{y_{j,calc}}$ – Intensity of calculated spectrum at energy j

$\boldsymbol{j}$ – Energy point number

$\boldsymbol{N}$ – Total number of energy points

$\boldsymbol{I}$ – Component number

$\boldsymbol{m}$ – Number of components

$\boldsymbol{I_{i,j}}$ – Normalized intensity of spectrum of component i at energy j

$\boldsymbol{x_i}$ – Proportion (fraction) of element as component i

3.3.3 Preparation of Standards

The height of the edge jump of each near-edge spectrum is proportional to the concentration of the examined element in the sample. Therefore, the concentration of each element in the unknown samples can be obtained by comparing the edge jump to the standard of known concentration. Standard solutions of 0.1mM arsenite and selenite were prepared fresh each time before data collection on the beamline. The near-edge spectra of the standard arsenite and selenite were recorded under the same conditions as the blood samples. The edge jumps of the standard arsenite and selenite were analyzed in the same manner as the experimental blood samples using EXAFSPAK.

Selenium and arsenic K near-edge standard spectra of different selenium species (e.g. selenite, selenate, $[(GS)_2AsSe]^-$, selenocystine, etc.) and arsenic species (arsenite, arsenate, $[(GS)_2AsSe]^-$, arsenic triglutathione, etc.) which possibly present in the samples were collected on the beamline . These standard spectra from the standard compounds were used to determine what species were present in our unknown samples.

Chapter 4: Disposition of Selenium after Injection of Selenite

Male New Zealand white rabbits (1.5-2kg) were selected for studying the fate of selenium after injection within a mammalian system. Selenite was injected via the ear vein as described in Chapter 3. Blood and cecotrope samples were collected after injection at different time intervals as described in Chapter 3.

4.1 Total Selenium Concentration in Blood after Injection of Selenite

Total concentrations of selenium in rabbit blood after injection of selenite were measured by comparing the edge jump of selenium K near-edge spectra to the standards of known concentration. Figure 4.1 shows the selenium concentration in whole blood (blue), red blood cell (red) and plasma (green) as well as the bars indicate data ± error. Errors were estimated using the signal amplitude, defined as the edge jump, and noise were determined by measuring the amplitude of the noise above the edge. While this is not a rigorous statistical treatment it gives a reasonable approximation of the uncertainty of the concentration estimates. There was little selenium present at time point 0 which was just before selenite injection, and that selenium probably came from the naturally present in the diet at a level of about 2.2 μM. Samples of whole blood, red blood cell and plasma 24hr after injection of selenite were also collected, but the concentrations were found to be very low. The selenium levels in plasma, whole blood and red cell were all very similar, and while there may be slightly more selenium in plasma, this difference

was close to our estimated error. The sample taken at 5min after injection showed the highest concentration of selenium in blood, and thereafter the concentrations of selenium gradually decreased, until 24hr after injection of selenite, selenium reached a level of about 3.5 μM.

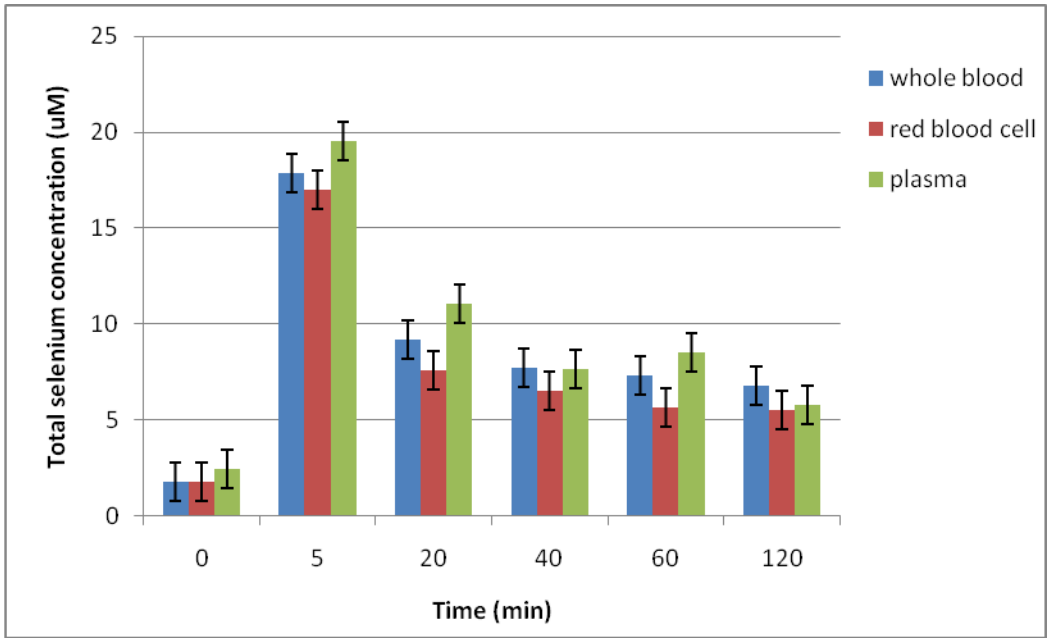

Figure 4.1 Total selenium concentrations (μM) in whole blood (blue), red blood cell (red) and plasma (green) collected from the rabbit after injection of selenite only, bars indicate data ± error; data were collected before injection, and at 5min, 20min, 40min, 1hr and 2hr after injection of selenite, respectively.

4.2 Speciation of Selenium in Blood after Injection of Selenite

Selenium K near-edge X-ray Absorption spectra of whole blood, plasma and red blood cell samples after injection of selenite were collected on the HXMA beamline at CLS. The selenium K near-edge spectra are sensitive to the local electronic environment of the selenium and oxidation states and thus can be used to identify the chemical forms of selenium present in each sample. In this study, selenate (SeO_4^{2-}), selenite (SeO_3^{2-}), elemental selenium (α-Se), selenomethionine (R-Se-R), selenodiglutathione (GS-Se-GS), selenyl sulfide (Cys-Se-S-Cys), selenocystine (CysSeSeCys) and inorganic selenide (HSe^-) were used to represent the selenium environments, respectively (Figure 4.2). Other selenium species were considered as potential models but the analysis showed insignificant fractions in all blood samples.

Least squares fit of the Se near-edge spectrum from whole blood 2h post injection to the sum of spectra of the standard model species are shown in Figure 4.3. Whole blood samples from other time points were fitted using the same standard species; a summary of the speciation results is shown in Table 4.1. Before injection of selenite, only two components—selenide and selenocystine were identified in whole blood sample. After injection of selenite, three components appeared to yield the best fits —selenide, selenite and elemental selenium. Elemental selenium (α-Se) was found to be the most abundant of all selenium compounds examined after injection, with a fraction varying from 60% to 51%. It is also possible that an unknown selenium species which has a similar spectrum to elemental selenium exists and this unknown species has a greater fraction of total

selenium in blood after injection of selenite. Among the samples collected from 5mins to 2hrs post injection, the fraction of selenite was quite stable; slightly fluctuate at 10%±1% of the total selenium content. However, the fraction of selenide was observed to increase over time and the fraction of elemental selenium decreases within 2h post injection of selenite.

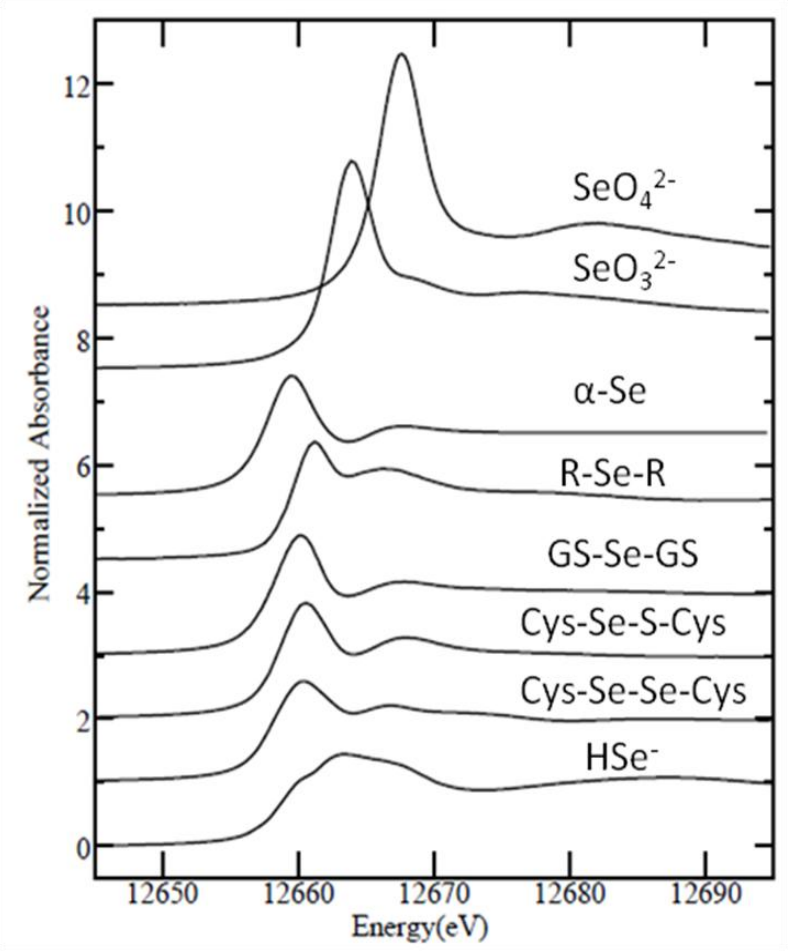

Figure 4.2 Selenium K near-edge spectra of standard selenium species.
SeO_4^{2-} (selenate), SeO_3^{2-} (selenite), α-Se(elemental selenium), R-Se-R (selenomethionine), GS-Se-GS (selenodiglutathione), CysSeSeCys (selenocystine), Cys-Se-S-Cys (selenyl sulfide) and HSe^- (selenide), respectively.

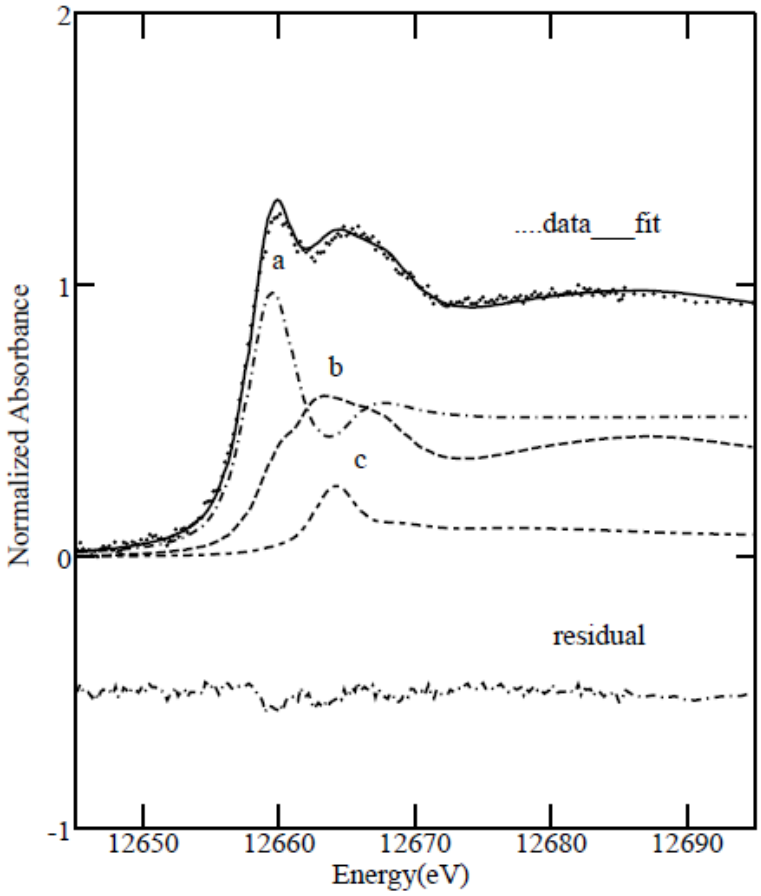

Figure 4.3 Least squares fit of the spectrum of rabbit whole blood sample 2hr after injection of selenite to the sum of spectra of standard selenium species. Figure shows the whole blood data (dotted line), the fit (solid line) and the individual components, scaled according to their contributions to the fit: a. α-Se b. HSe^- c. SeO_3^{2-}. The residual is shown offset below. Numerical results are shown in Table 4.1.

Table 4.1 Percentage of selenium as each selenium species in rabbit whole blood samples after injection of selenite.

Time	**HSe^-**	**SeO_3^{2-}**	**α-Se**	**CysSeSeCys**	**CysSeSCyS**
0	47(7)	—	—	53(7)	—*
5min	28(5)	11(2)	60(3)	—	—
20min	31(5)	11(3)	58(3)	—	—
40min	32(5)	11(3)	57(3)	—	—
1hr	36(6)	9(3)	55(3)	—	—
2hr	41(4)	9(2)	51(2)	—	—

Se K near-edge fitting results from whole blood from the rabbit injected with selenite, samples represent whole blood collected before injection, 5min, 20min, 40min, 1h and 2h post injection of selenite, respectively. Values derived from percentage contributions of spectra of standards to the best fit of the sample spectra. Figures in parenthesis show three times estimated standard deviation. Selenide, selenite, elemental selenium and selenocystine are represented by HSe^-, SeO_3^{2-}, α-Se and CysSeSeCys, respectively.

* Note that this component was observed in plasma. Presumably it is not observed here because of the higher relative errors and correlation with CySSeSeCyS in the fit.

The Se K near-edge spectra of the red blood cell fractions after injection of selenite within 2h were also collected. Least squares fit of the red blood cell spectrum 2h post injection of selenite to the sum of spectra of standard species is shown in Figure 4.4. The remaining time points for the red blood cell fractions were fitted in the same manner, the results of which are shown in Table 4.2.

Before injection of selenite, two components were found to obtain the best fit (selenide and selenocystine) in red blood cell. After injection of selenite, three components (selenide, selenite and elemental selenium) appeared to obtain the best fits in red blood cells. Elemental selenium and selenide were found to be the most abundant of all selenium species. At 5min time point, the red blood cell had the highest fraction of elemental selenium and the least fraction of selenide. Among all the samples collected within 2hrs post injection, the fraction of selenite was quite stable, slightly fluctuating around 8%±2% of the total selenium content.

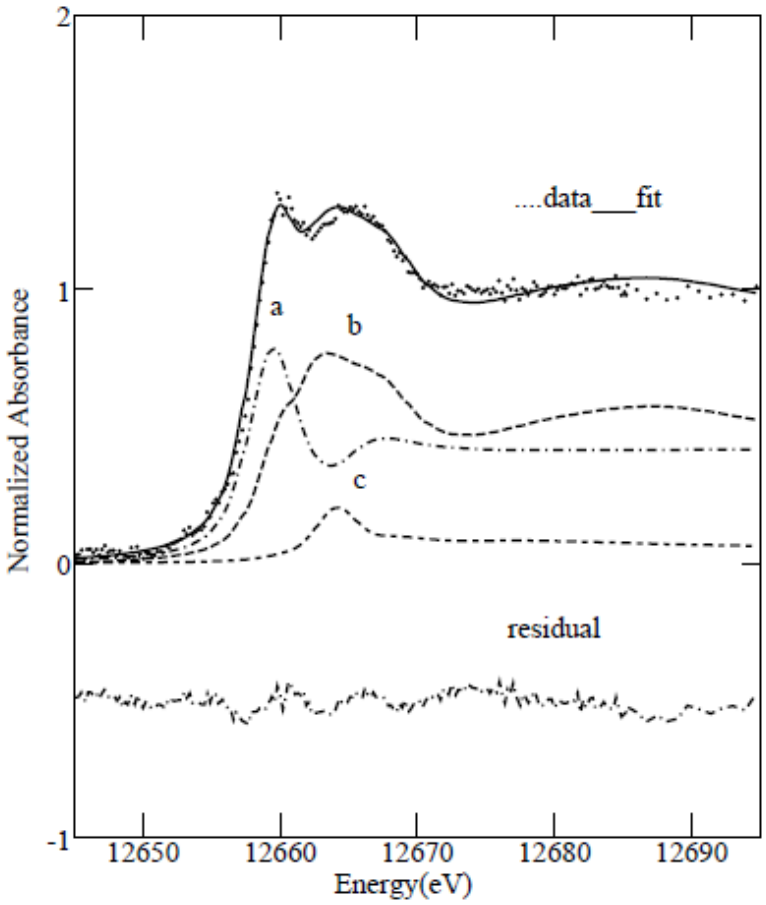

Figure 4.4 Least squares fit of the spectrum of rabbit red blood cells sample 2hr post injection of selenite to the sum of spectra of standard selenium species. Figure shows the whole blood data (dotted line), the fit to the data (solid line) and the individual components, scaled according to their contributions to the fit: a. α-Se b. HSe^- c. SeO_3^{2-}. The residual is shown offset below. Numerical results are shown in Table 4.2.

Table 4.2 Percentage of selenium as each selenium species in rabbit red blood cell samples after injection of selenite.

Sample	**HSe^-**	**SeO_3^{2-}**	**α-Se**	**CysSeSeCys**
0	46(6)	—	—	54(7)
5min	30(3)	9(1)	61(2)	—
20min	46(4)	8(2)	46(2)	—
40min	40(4)	10(2)	50(2)	—
1hr	45(4)	7(2)	47(2)	—
2hr	53(5)	7(3)	41(3)	—

Se K near-edge fitting results from whole blood from the rabbit injected with selenite, samples represents red blood cell collected before injection, 5min, 20min, 40min, 1h and 2h post injection of selenite, respectively. Values derived from percentage contributions of spectra of standards to the best fit of the sample spectra. Figures in parenthesis show three times estimated standard deviation. Selenide, selenite, elemental selenium and selenocystine are represented by HSe^-, SeO_3^{2-}, α-Se and CysSeSeCys, respectively.

The Se K near-edge spectra of the plasma fractions after injection of selenite within 2h were also collected. Least squares fit of the plasma spectrum 2h post injection of selenite to the sum of spectra of standard species is shown in Figure 4.5. The remaining time points for the plasma fractions were fitted in the same manner; the results of which are shown in Table 4.3.

Before injection of selenite, three components were found to obtain the best fit (selenite, selenocystine and selenyl sulfide) in plasma. After injection of selenite, two components (selenite and elemental selenium) appeared to yield the best fits in plasma. At 5min time point, plasma had highest fraction of elemental selenium (79%) and the lowest fraction of selenide (21%). From 20min to 2hr post injection of selenite, the fractions of elemental selenium in plasma decreased and stabilized at around 77%±1% of the total selenium content. Meanwhile, the fractions of selenide increased and stabilized at around 23%±1% of total selenium. Inorganic selenide was not expected to be found in plasma, because plasma is an oxidizing environment. (Schafer and Buettner, 2001; Ingrid *et al.*, 1998).

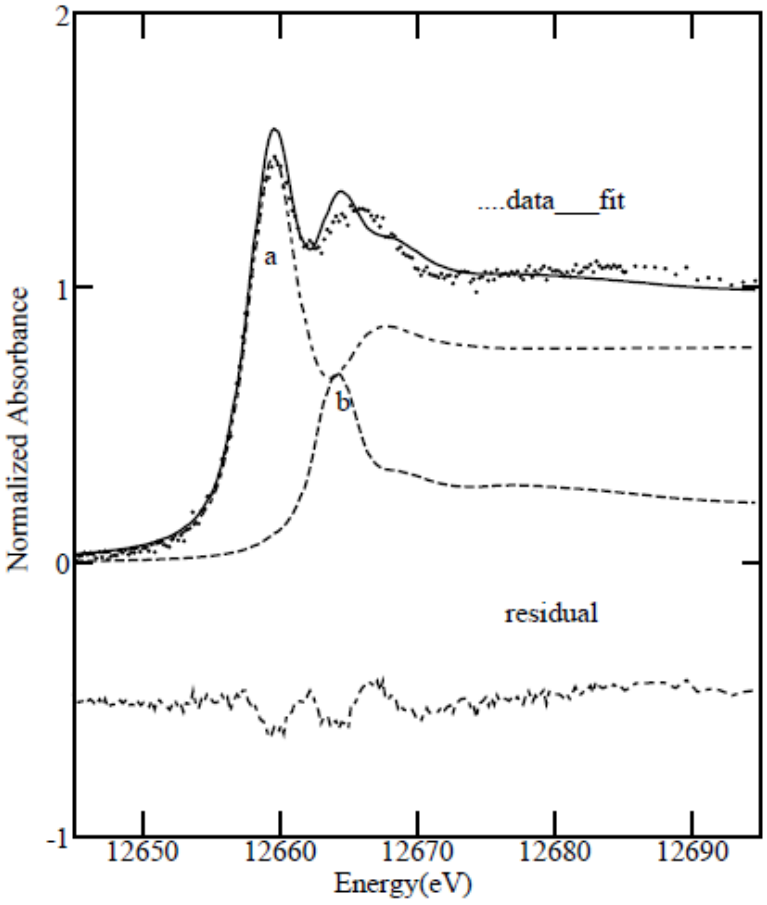

Figure 4.5 Least squares fit of the spectrum of rabbit plasma sample 2hr post injection of selenite to the sum of spectra of standard selenium species. Figure shows the plasma data (dotted line), the fit to the data (solid line) and the individual components, scaled according to their contributions to the fit: a. Se^0 b.SeO_3^{2-}. The residual is shown offset below. Numerical results are shown in Table 4.3.

Table 4.3 Percentage of selenium as each selenium species in rabbit plasma samples after injection of selenite.

Sample	**SeO_3^{2-}**	**α-Se**	**CysSeSeCys**	**CysSeSCys**
0	24(2)	—	49(19)	27(18)
5min	21(1)	79(2)	—	—
20min	24(1)	76(2)	—	—
40min	23(1)	77(2)	—	—
1hr	24(1)	76(2)	—	—
2hr	23(1)	77(2)	—	—

Se K near-edge fitting results from whole blood from the rabbit injected with selenite, samples represents plasma collected before injection, 5min, 20min, 40min, 1h and 2h post injection of selenite, respectively. Values derived from percentage contributions of spectra of standards to the best fit of the sample spectra. Figures in parenthesis show three times estimated standard deviation. Selenite, elemental selenium selenocystine, selenyl sulfide are represented by SeO_3^{2-}, α-Se, CysSeSeCys and Cys-Se-S-Cys, respectively.

4.3 Speciation of Selenium in Cecotrope after Injection of Selenite

The Se K-near edge spectra of rabbit cecotrope sample 24hr post injection of selenite was also collected. Spectrum of cecotrope was fitted to the sum of spectra of standard selenium species (Figure 4.6), five components (selenodiglutathione, selenide, selenite, selenate and selenomethionine) appeared to yield the best fit to data. A species resembling GS-Se-GS was found to be the most abundant species comprising 54% of total selenium content in cecotrope. Organic selenide (R-Se-R) was present in smaller amount with a fraction of 22% of total selenium, and inorganic selenide was present at a fraction of 19% of total selenium. In addition, inorganic selenide (HSe^-) was found in cecotrope, this is probably because cecotrope is a product from cecum, and cecum is an anaerobic environment so that HSe^- can exist.

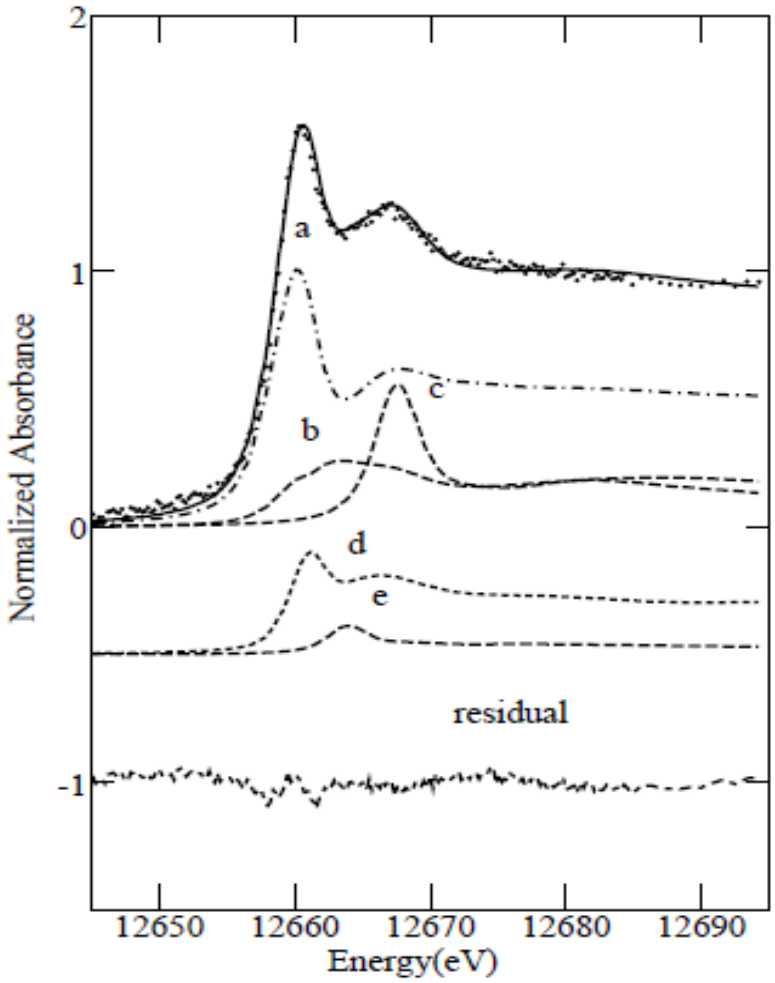

Figure 4.6 Least squares fit of the spectrum of rabbit cecotrope sample 24hr post injection of selenite to the sum of spectra of standard selenium species. Figure shows the cecotrope data (dotted line), the fit (solid line) and the individual components, scaled according to their contributions to the fit: a. GS-Se-GS (selenodiglutathione) b. HSe^- (selenide) c. SeO_3^{2-} (selenite), d. R-Se-R (selenomethionine), e. $SeO4^{2-}$ (Selenate). The residual is shown offset below.

4.4 Discussion

The above results show that after injection of selenite into rabbit, blood selenium levels in plasma, red cell and whole blood were all very similar. After injection of selenite, HSe^- and α-Se were found to be the most abundant selenium species in red blood cells and whole blood samples within 2h post injection. It was reported that nano-particulate elemental selenium can be formed by the reaction of selenite and glutathione (JS Zhang *et al.*, 2001). It was also believed that nano-size elemental selenium had a lower toxicity than selenite. *In vitro* studies had shown that the detoxification of selenite involves reactions with thiol-containing molecules like glutathione, directing the production of intermediate metabolites hydrogen selenide (HSe^-) and finally to elemental selenium (H.E. Ganther, 1968 and J.L. Kice, 1980). However, the mechanism of how elemental Se was formed in blood remains unknown. Our experimental results demonstrate that elemental selenium α-Se is rapidly formed in rabbit blood after injection of selenite. It is widely known that there are selenoproteins in plasma and selenoprotein P is the most abundant. It includes 10 selenocysteine residues (Se-Cys). Recently, researchers have found that selenoprotein P plays important roles in selenium homeostasis and transport in mammals (Burk *et al.*, 2009). In our experiments for time zero (before injection of selenite), the selenium in plasma was likely to be predominantly selenoprotein P. Thus, the observation of Cys-S-Se-Cys suggested that this form is predominant in selenoprotein P and in other selenoproteins. Our observation of selenite in

plasma is also consistent with prior work as a Japanese group has indicated that free selenite is normally present in plasma (Suzuki and Itoh, 1996).

24hr post injection of selenite, a small fraction of selenite was detected in cecotrope sample. This indicates the selenite injected to the rabbit has largely been removed from blood. After digestion and metabolism, selenomethionine and selenodiglutathione were found to be the most abundant species in cecotrope.

Chapter 5:

Disposition of Arsenic after injection of Arsenite

Male New Zealand white rabbits (1.5-2kg) were selected for studying the fate of arsenic after injection within a mammalian system. Arenite was injected to the rabbit as described in Chapter 3. Blood and cecotrope samples were collected after injection at different time intervals as described in Chapter 3.

5.1 Total arsenic concentration in blood after injection of arsenite

Total concentrations of arsenic in rabbit blood after injection of arsenite were measured by comparing the edge jump of arsenic K near-edge spectra to standards of known concentration. Figure 5.1 shows the total arsenic concentration in whole blood (blue), red blood cell (red) and plasma (green) as well as the bars indicating data $\pm$ error. Errors were estimated using the signal amplitude, defined as the edge jump, and noise determined by measuring the amplitude of the noise above the edge. While this is not a rigorous statistical treatment it gives a reasonable approximation of the uncertainty of the concentration estimates. Time 0 stands for total arsenic concentration before injection. From figure 5.1, there was no measureable arsenic in rabbit blood samples before injection. Samples of whole blood, red blood cell and plasma 4h and 24h after injection of arsenite were also collected. The concentration of arsenic in blood sample 4h after injection was as low as $0.2 \pm 0.05\,\mu M$, while the total concentration of arsenic in blood 24h post injection was 0. At each time point in Figure 5.1, more arsenic was observed in red

blood cell fraction compared with whole blood or plasma. The highest concentration of arsenic in blood was observed 5min post injection, with the concentration of arsenic gradually decreasing over time. Within 24h post injection of arsenite, the arsenic content was largely cleared from the blood.

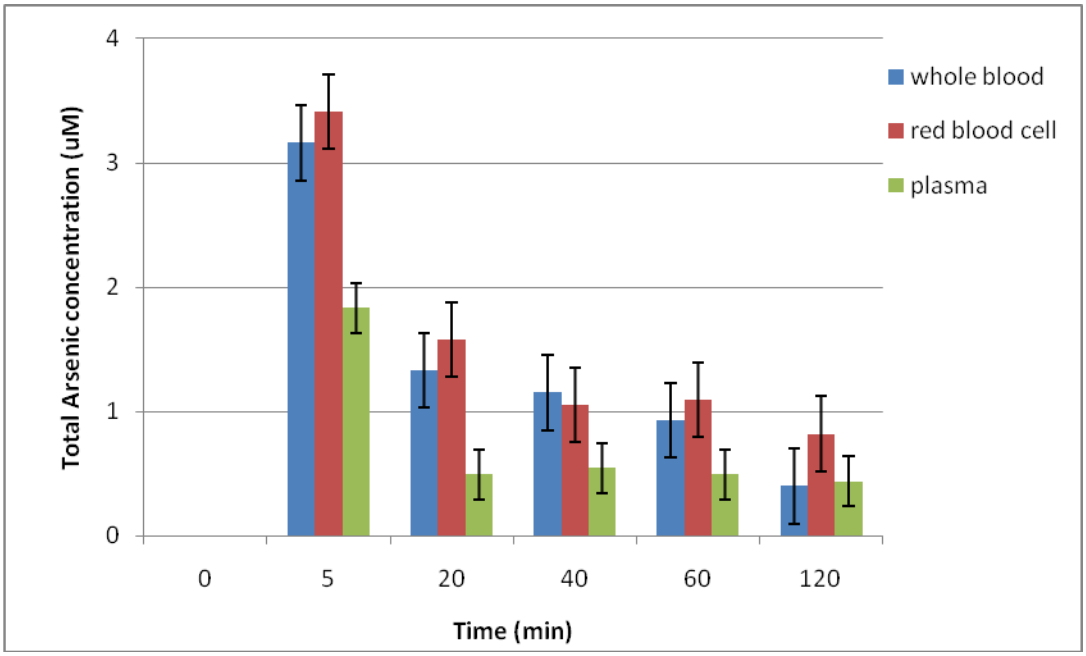

Figure 5.1 Total arsenic concentrations (μM) in whole rabbit blood (blue), red blood cells (red) and plasma (green) after injection of arsenite only. Error bars indicate data ± error; data were collected before injection and at 5min, 20min, 40min, 1h and 2h post injection of arsenite, respectively.

5.2 Speciation of Arsenic in blood after injection of Arsenite

Arsenic K near-edge X-ray absorption spectra of whole blood, plasma and red blood cells sample after injection of arsenite were collected on the HXMA beamline at CLS. The arsenic K-edge spectra are sensitive to the local electronic environment of the arsenic and oxidation states and this technique can be used to identify the chemical forms of arsenic present in each sample. In this study, arsenite (AsO_3^{3-}), arsenic triglutathione [$As(GS)_3$] and a sulfur coordinated MMA^{III} (monomethylarsonous acid) as the form of [$CH_3As(HlipS_2)$] where $HlipS_2^{2-}$ means the reduced lipoic acid were used as representative models for the potential chemical forms of arsenic (Figure 5.2). The spectra of whole blood collected after injection of arsenite show variability in the arsenic species present (Figure 5.3). Least squares fit of the As near-edge spectrum from whole blood 5min after injection fitted to the sum of spectra of the standard model species is shown in Figure 5.3. Whole blood samples from other time points were fitted using the same standard species; a summary of the speciation results are shown in Table 5.1. Three components appeared to yield the best fits to the data, $As(GS)_3$, arsenite and $CH_3As(HlipS_2)$. $CH_3As(HlipS_2)$ was found to be the most abundant of all arsenic species, with the fraction varying from 45% to 94% of the total arsenic content in the blood. Comparing all samples collected between 5min to 2h post injection, the 5min time point had the greatest fraction of arsenite, and the lowest fraction of $CH_3As(HlipS_2)$. At later time points, the fractions of arsenite decreased and the fractions of $CH_3As(HlipS_2)$ increased. These results indicate that the arsenite injected into blood becomes methylated,

forming $CH_3As(HlipS_2)$, with the formation of $As(GS)_3$ existing as an intermediate during this biotransformation. The concentrations of As in whole blood samples collected 40min post injection and later were low, resulting in less signal in the As K near-edge spectra. The low As concentrations in these later time points made it difficult to obtain accurate fractions for individual species, however, the major species being $CH_3As(HlipS_2)$ is unmistakable.

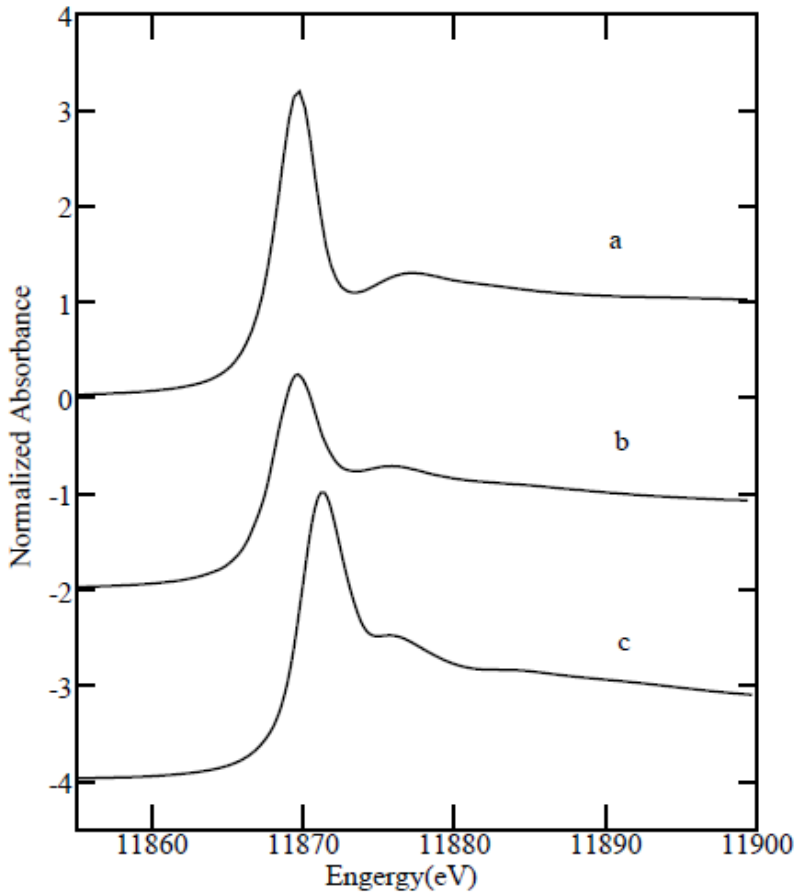

Figure 5.2 As K near-edge spectra of standard arsenic species.
a. $As(GS)_3$ b. $CH_3As(HlipS_2)$ c. AsO_3^{3-}

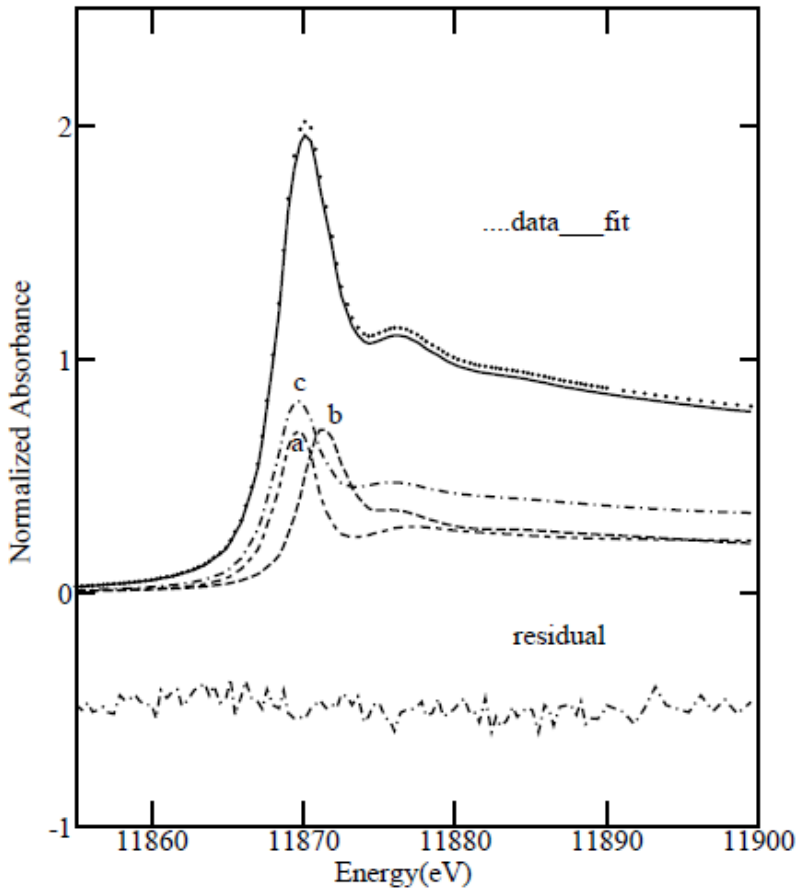

Figure 5.3 Least squares fit of the As K near-edge spectrum of rabbit whole blood 5min post injection of arsenite, fitting to the sum of spectra of standard arsenic species. Represented is whole blood data (dotted line), the fit to the data (solid line) and individual components, scaled according to their contributions to the fit: a. $As(GS)_3$ b. arsenite c. $CH_3As(HlipS_2)$. The residual is shown offset below. Numerical results are shown in Table 5.1.

Table 5.1 Percentage of arsenic as each arsenic species in rabbit whole blood samples after injection of arsenite.

Time	**$As(GS)_3$**	**AsO_3^{3-}**	**$CH_3As(HlipS_2)$**
5min	27(12)	28(5)	45(17)
20min	—	11(8)	68(9)
40min	—	10(8)	90(13)
1hr*	—	—	92(10)
2hr*	—	—	94(13)

As K near-edge fitting results from whole blood from the rabbit injected with arsenite, samples represent whole blood collected 5min, 20min, 40min, 1h and 2h post injection of arsenite, respectively. Values derived from percentage contributions of spectra of standards to the best fit of the sample spectra. Figures in parenthesis show three times standard deviation. Tri-glutathione arsenic, arsenite, and the sulfur coordinated MMA^{III} are represented by $As(GS)_3$, AsO_3^{3-} and $CH_3As(HlipS_2)$, respectively. * indicates the sample is dilute resulting in poor data quality precluding accurate analysis, and only the major component is therefore determined.

The As K near-edge spectra of the red blood cell fractions after injection of arsenite within 2h were also collected. Least squares fit of the red blood cell spectrum 5min post injection of arsenite was fitted to the sum of spectra of standard species (Figure 5.4). The remaining time points for the red blood cell fractions were fitted in the same manner; the results of which are shown in Table 5.2. Similar to the whole blood data, three components [$As(GS)_3$, arsenite and $CH_3As(HlipS_2)$] appeared to yield the best fits, for the sample 5min post injection. Across all time points studied, $CH_3As(HlipS_2)$ was found to be the most abundant of all arsenic species, with this species comprising 35% to 88% of the total As content in red blood cells. Arsenite was only identified 5min post injection, and comprised a small fraction of the total (6%). From 5min to 20min post injection, the fractions of $As(GS)_3$ decreased and finally disappeared at later time points while the fractions of $CH_3As(HlipS_2)$ increased and became the only As species in red blood cell.

The concentration of arsenic in red blood cells collected 40min post injection and later was low, resulting in lower signals in the As K near-edge spectra. Therefore, it is difficult to obtain accurate fractions for individual species; however, the major species of $CH_3As(HlipS_2)$ has been detected.

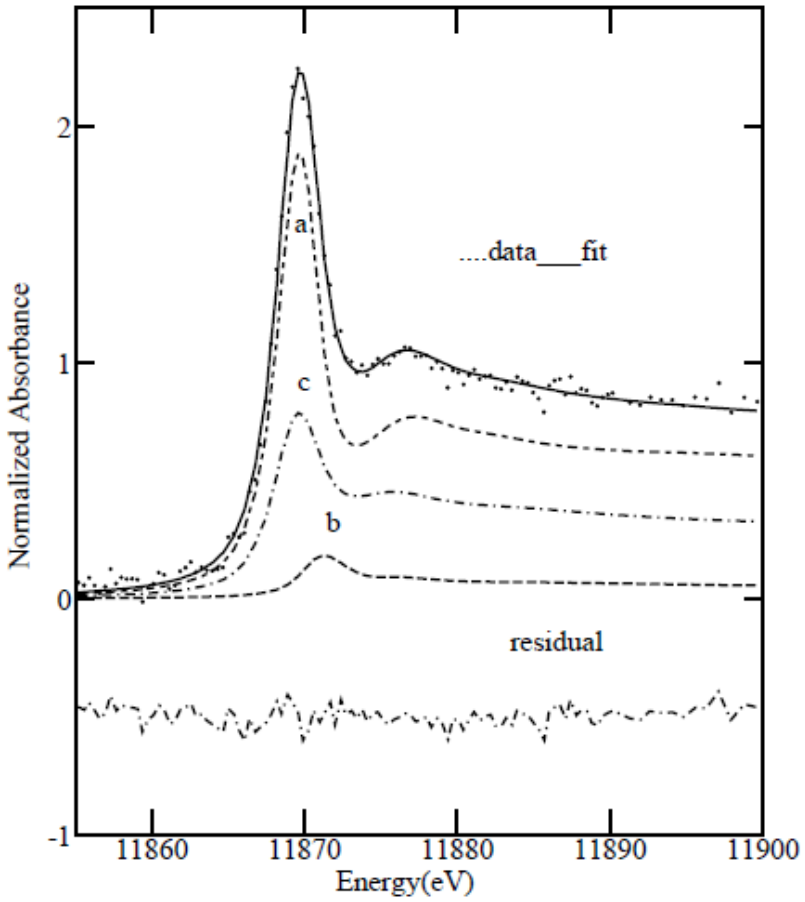

Figure 5.4 Least squares fit of the As K near-edge spectrum of red blood cells 5min post injection of arsenite to the sum of spectra of standard arsenic species. Shown are the red blood cell data (dotted line), the fit (solid line) and the individual components, scaled according to their contributions to the fit: a. $As(GS)_3$ b. arsenite c. $CH_3As(HlipS_2)$. The residual is shown offset below. Numerical results are shown in Table 5.2.

Table 5.2 Percentage of arsenic as each arsenic species in rabbit red blood cells after injection of arsenite.

Sample	**$As(GS)_3$**	**AsO_3^{3-}**	**$CH_3As(HlipS_2)$**
5min	59(10)	6(4)	35(14)
20min	34(17)	—	66(19)
40min*	—	—	84(5)
1hr*	—	—	86(7)
2hr*	—	—	88(10)

As K near-edge fitting results from red blood cells isolated from the rabbit injected with arsenite, samples represent red blood cells 5min, 20min, 40min, 1h and 2h post injection of arsenite, respectively. Values derived from percentage contributions of spectra of standards to the best fit of the sample spectra. Figures in parenthesis show three times standard deviation. Tri-glutathione arsenic, arsenite, and the sulfur coordinated MMA^{III} are represented by $As(GS)_3$, AsO_3^{3-} and $CH_3As(HlipS_2)$, respectively. * indicates that sample is dilute resulting in poor data quality precluding accurate analysis, and only the major component is therefore determined.

The As K near-edge spectra of plasma factions after injection of arsenite within 2h were also collected. Least squares fit of the plasma spectrum 5min post injection of arsenite was fitted to the sum of spectra of standard species. Arsenite and $As(GS)_3$ appear to yield the best fit (Figure 5.5). The remaining time points for plasma fractions were fitted in the same manner; the results of which are shown in Table 5.3. Across all time points studied arsenite was found to be the most abundant of all arsenic species between 5min and 40min post injection, with this species comprising 88% to 52% of the total As content in plasma. Also, more arsenite was observed in plasma fractions compared with whole blood or plasma at each time point.

The concentrations of arsenic in plasma collected 1h post injection and later were low, resulting in lower signals in the As K near-edge spectra. Therefore, it is difficult to obtain accurate fractions for individual species; however, the major species of $CH_3As(HlipS_2)$ has been detected.

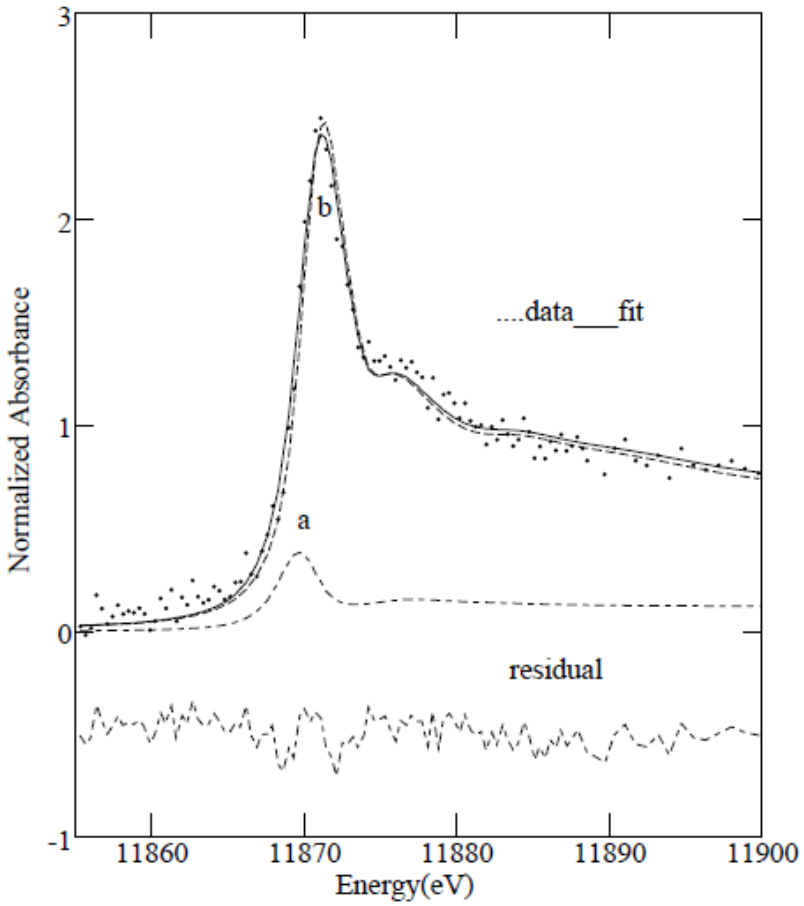

Figure 5.5 Least squares fit of the As K near-edge spectrum of plasma 5min post injection of arsenite to the sum of spectra of standard arsenic species. Shown are the plasma data (dotted line), the fit (solid line) and the individual components, scaled according to their contributions to the fit: a. $As(GS)_3$ b. arsenite. The residual is shown offset below. Numerical results are shown in Table 5.3.

Table 5.3 Percentage of arsenic as each arsenic species in plasma fractions after injection of arsenite.

Sample	**$As(GS)_3$**	**AsO_3^{3-}**	**$CH_3As(HlipS_2)$**
5min	12(5)	88(5)	—
20min	19(18)	81(18)	—
40min	—	52(25)	48(29)
1hr*	—	—	55(15)
2hr*	—	—	60(13)

As K near-edge fitting results from plasma isolated from the rabbit injected with arsenite, samples represent plasma 5min, 20min, 40min, 1h and 2h post injection of arsenite, respectively. Values derived from percentage contributions of spectra of standards to the best fit of the sample spectra. Figures in parenthesis show three times standard deviation. Tri-glutathione arsenic, arsenite, and the sulfur coordinated MMA^{III} are represented by $As(GS)_3$, AsO_3^{3-} and $CH_3As(HlipS_2)$, respectively. * indicates that sample is dilute resulting in poor data quality precluding accurate analysis, and only the major component is therefore determined.

5.3 Speciation of arsenc in cecotrope after injection of arsenite

The As K near-edge spectrum of cecotrope 24h post injection of arsenite was also collected. Least squares fit of the cecotrope spectrum was fitted to the sum of spectra of standard species (Figure 5.6). Arsenite and $CH_3As(HlipS_2)$ appeared to yield the best fit and the results are shown in Table 5.4. $CH_3As(HlipS_2)$ was found to be the most abundant of all arsenic species comprising 84% of total arsenic content in cecotrope.

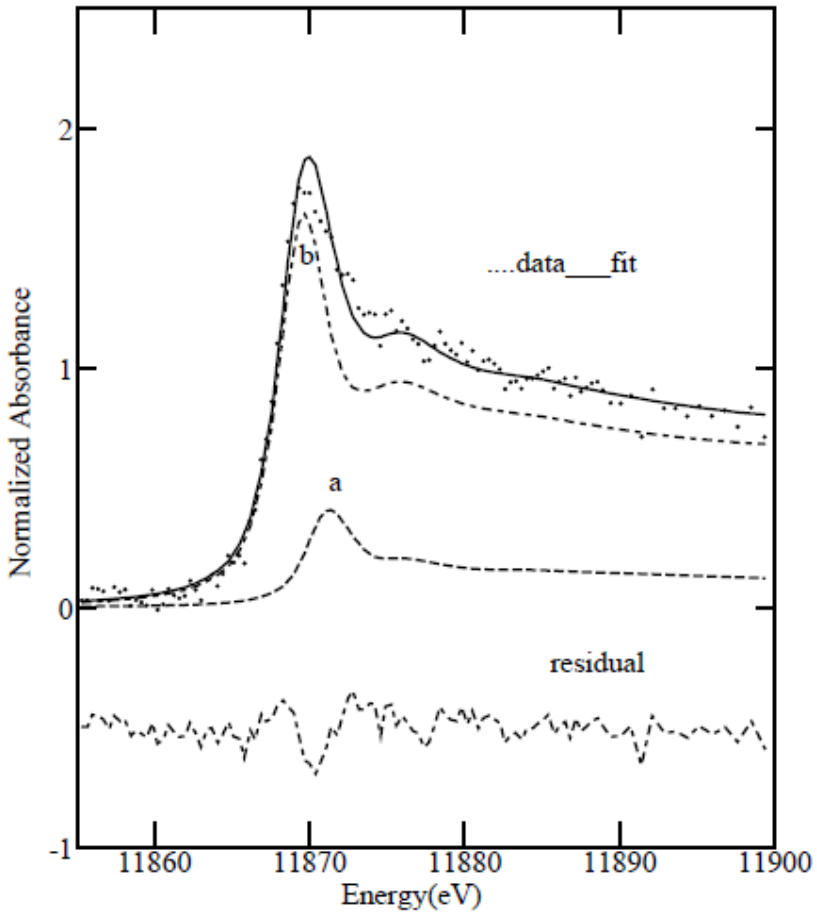

Figure 5.6 Least squares fit of the As K near-edge spectrum of cecotrope 24h post injection of arsenite to the sum of spectra of standard arsenic species. Shown are the plasma data (dotted line), the fit (solid line) and the individual components, scaled according to their contributions to the fit: a. arsenite b. $CH_3As(HlipS_2)$. The residual is shown offset below. Numerical results are shown in Table 5.4.

Table 5.4 Percentage of arsenic as each arsenic species in rabbit cecotrope sample after injection of arsenite.

Sample	**AsO_3^{3-}**	**$CH_3As(HlipS_2)$**
As_cecotrope	16(5)	84(6)

As K near-edge fitting results of cecotrope from the rabbit injected with arsenite. Values derived from percentage contributions of spectra of standards to the best fit of the sample spectra. Figures in parenthesis show three times standard deviation. Tri-glutathione arsenic, arsenite, and the sulfur coordinated MMA^{III} are represented by AsO_3^{3-} and $CH_3As(HlipS_2)$, respectively.

5.4 Discussion

The above results show that after injection of arsenite into rabbit, blood arsenic accumulates in red blood cells as opposed to plasma. In the blood, arsenic was mostly bound to plasma thiols most likely being transformed to $As(GS)_3$ within minutes of injection. The generally accepted pathway for biotransformation of inorganic arsenic is methylation (Challenger, F. 1945), and the methylation of arsenic in mammals is thought to take place in liver. A novel metabolic arsenic pathway, proposed by Hayakawa (Hayakawa *et al.,* 2005), indicated that $As(GS)_3$ forms as an intermediate during arsenic biotransformation; however, this proposal remains controversial. Our experiment results demonstrate that $As(GS)_3$ is one of the main metabolites in the blood within 5-20mins after injection of arsenite. Within 20min post injection, the methylated species $CH_3As(HlipS_2)$ is detected in whole blood, red blood cells and plasma fractions. This indicates that $As(GS)_3$ becomes methylated forming a $CH_3As(HlipS_2)$ species (likely $CH_3As^{III}(GS)_2$). Although the detoxification pathway indicates that DMA(V) and MMA(V) are the end products of arsenic biotransformation, no evidence of those species have been detected in our experiments and longer exposures to arsenite might be needed to detect these. However, arsenic was rapidly eliminated and quickly became undetectable in our experiments.

Chapter 6:

Disposition of Selenium and Arsenic after Injection of Selenite and Arsenite

Two male New Zealand white rabbits (1.5-2kg) were selected for studying the fate of arsenic and selenium after injection of arsenite and selenite within a mammalian system. Arsenite and selenite were injected to the rabbits as described in Chapter 3. The first rabbit was injected with prepared arsenite followed by selenite via ear vain. The second rabbit was injected with prepared selenite followed by arsenite. Blood and cecotrope samples were collected after injection at different time intervals as described in Chapter 3.

6.1 Selenium and Arsenic Levels in Blood

Arsenite and selenite were both administered to rabbits. Two different experiments were done – in the first which arsenite was given three minutes before selenite, and in the second selenite was given three minutes before arsenite.

6.1 .1 Total Selenium and Arsenic Concentration in Blood after Injection of Arsenite followed by Selenite

Total concentrations of selenium in rabbit blood after injection of arsenite and then followed by selenite 3min later were measured by comparing the edge jumps of the selenium and arsenic K near-edge spectra to those of standards of known concentrations. Figure 6.1 shows the total selenium concentration in whole blood (blue), red blood cell

(red) and plasma (green) as well as the bars indicate data ± error. Errors were estimated as peak-peak noise amplitude using a spectroscopically unstructured region above the absorption edge and approximately correspond to a 99% confidence limit. While this is not a rigorous statistical treatment it gives a reasonable approximation of the uncertainties associated with concentrations estimates. There was found to be a low concentration of selenium present at time point 0, which is just before the injection, and this probably corresponds to functional selenium from that naturally present in the diet at a level of about 2.0 μM. Samples of whole blood, red blood cell and plasma 24h after injection of arsenite followed by selenite were also collected, and the selenium level was found to be as low as 1.7 ± 0.4 μM. The selenium levels in plasma, whole blood and red blood cell were all very similar, and while slightly more selenium was found in plasma, the difference is close to our estimated error. The highest concentration of selenium in blood was observed 5min post injection, with the concentration of selenium gradually decreasing over time.

Figure 6.2 shows the total arsenic concentrations in whole blood (blue), red blood cell (red) and plasma (green) and the bars indicate data ± error. The arsenic concentrations in blood within 2h post injection were obtained as the same manner as selenium levels. From figure 6.2, there was no measureable arsenic in rabbit blood samples before injection. 24h post injection of arsenite followed by selenite, no significant amount of arsenic was detected. This indicates the arsenic content was largely cleared from blood 24h after injection. At each time point in Figure 6.2, more arsenic is

observed in red blood cell fractions compared with whole blood or plasma. The sample taken at 5min after injection shows the highest concentration of arsenic in blood, and thereafter the concentrations of arsenic gradually decrease, until 24hr after injection, the arsenic content has been largely cleared from the blood.

Figures 6.1 and 6.2 indicate that at each time point post injection, blood selenium levels are much higher than arsenic levels. The likely reason for this is that arsenite is cleared from blood rapidly and upon selenite injection 3min later; most arsenic has already been removed from blood. Secondly, our experimental results indicate that arsenite has a higher elimination rate than selenium.

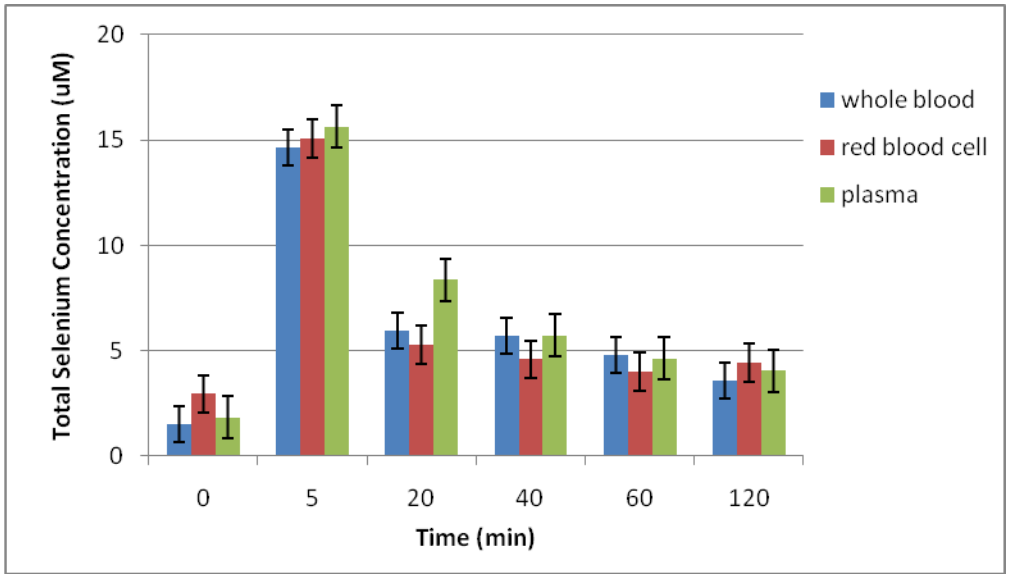

Figure 6.1 Total selenium concentrations (μM) in whole blood (blue), red blood cell (red) and plasma (green) collected from the rabbit after injection of arsenite followed by selenite, bars indicate data ± error, data were collected before injection, and at 5min, 20min, 40min, 1hr and 2hr post injection of arsenite followed by selenite, respectively.

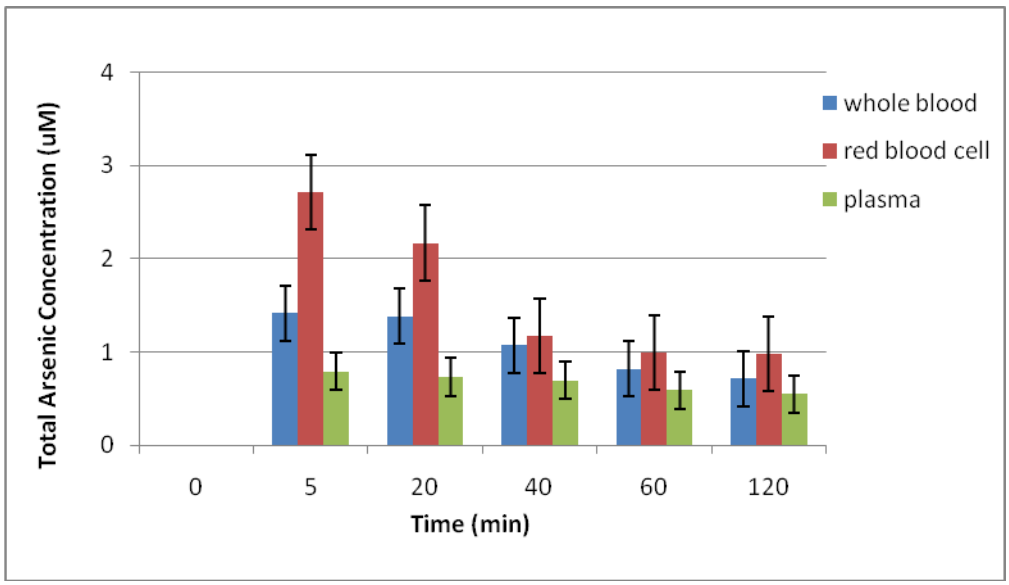

Figure 6.2 Total arsenic concentrations (μM) in whole blood (blue), red blood cell (red) and plasma (green) collected from the rabbit after injection of arsenite followed by selenite, bars indicate data ± error, data were collected before injection, and at 5min, 20min, 40min, 1hr and 2hr after injection of arsenite followed by selenite, respectively.

6.1.2 Total Selenium and Arsenic Concentration in Blood after Injection of Selenite followed by Arsenite

Total concentrations of selenium in rabbit blood after injection of selenite and 3min later followed by arsenite were measured by comparing the edge jump of either selenium or arsenic K near-edge spectra to standards of known concentrations. Figure 6.3 shows the total selenium concentration and Figure 6.4 shows the total arsenic concentration in whole blood (blue), red blood cell (red), plasma (green) and the bars indicate data ± error. Both selenium and arsenic concentrations are measured in the same manner. Before injection, a level of 2.2 μM of selenium was detected. No observable levels of arsenic were present in blood before injection. The highest concentrations of both selenium and arsenic in blood were observed 5min post injection, with the concentration of both gradually decreasing over time. Within 24h post injection, the selenium content reached a level of 1.2 ± 0.5 μM while the arsenic content was largely cleared from the blood. The selenium levels in plasma, whole blood and red blood cell were all very similar, and while there may be slightly more selenium in plasma (Figure 6.3), this difference is close to our estimated error. At each time point in Figure 6.4, more arsenic was observed in red blood cell fractions compared with whole blood or plasma.

From Figure 6.3 and 6.4, the selenium levels were consistently higher than the arsenic levels at all time points. This indicates that irrespective of whether arsenite is injected before or after selenite, arsenic has a higher elimination rate and it can be removed from blood faster than selenium.

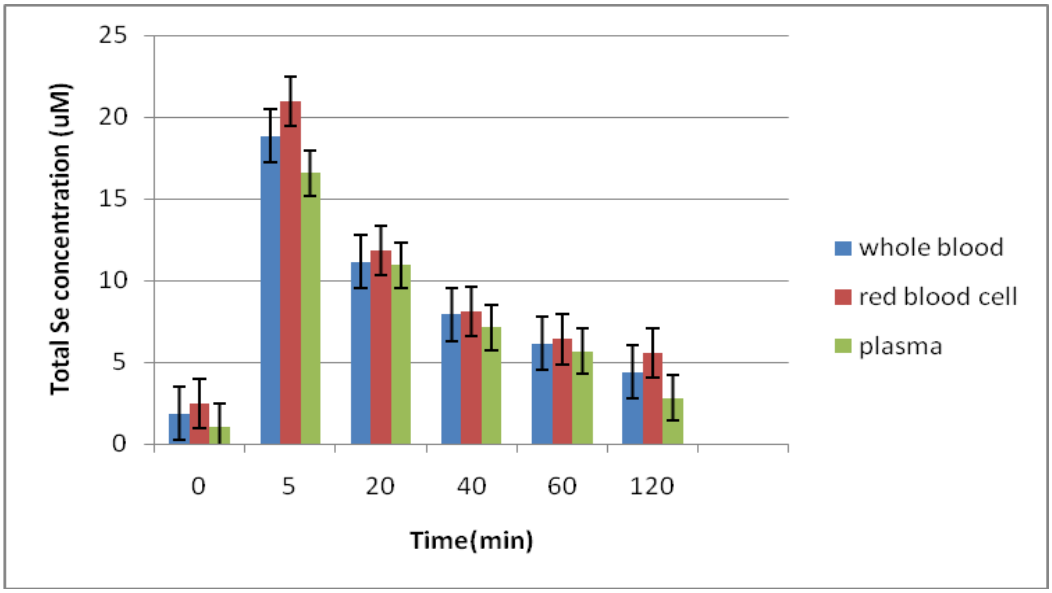

Figure 6.3 Total selenium concentrations (μM) in whole blood (blue), red blood cell (red) and plasma (green) collected from the rabbit after injection of selenite followed by arsenite, bars indicate data ± error, data were collected before injection and at 5min, 20min, 40min, 1hr and 2hr after injection of selenite followed by arsenite, respectively.

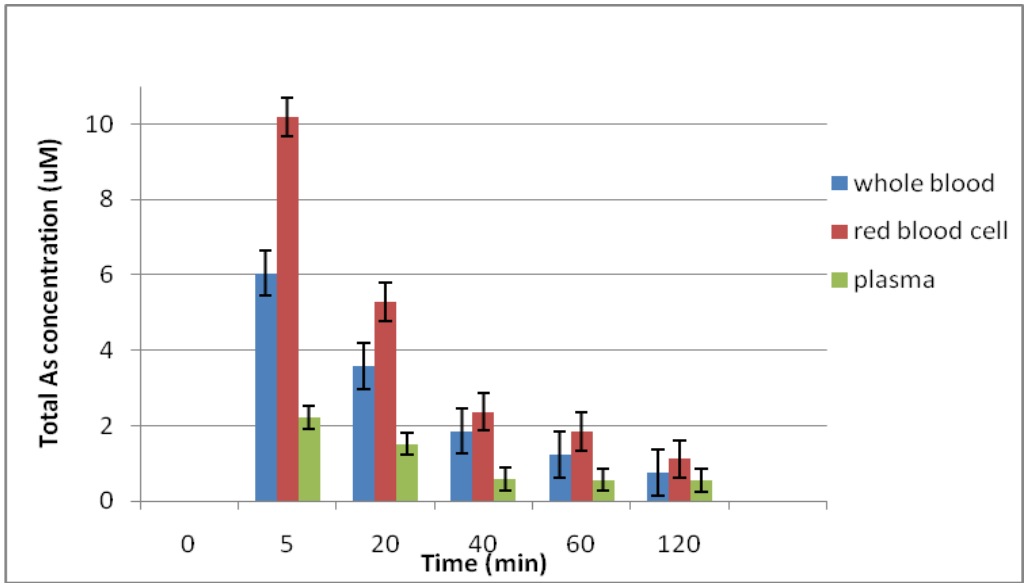

Figure 6.4 Total arsenic concentrations (μM) in whole blood (blue), red blood cell (red) and plasma (green) collected from the rabbit after injection of selenite followed by arsenite, bars indicate data ± error, data were collected before injection, and at 5min, 20min, 40min, 1hr and 2hr after injection of selenite followed by arsenite, respectively.

6.2 Speciation of Arsenic and Selenium after Injection of Selenite and Arsenite

Both arsenic and selenium K near-edge spectra of whole blood, red blood cells and plasma samples after injection of arsenite and selenite were collected. The arsenic or selenium K-edge spectra are sensitive to the local electronic environment of the arsenic or selenium and their oxidation states, and this technique can be used to identify the chemical forms of arsenic and selenium present in each sample. In this study, Figure 6.5 shows representative models for the potential chemical forms of arsenic and Figure 6.6 shows the potential selenium models. Other arsenic or selenium species were also considered as potential models but the analysis shows insignificant fractions in all blood samples.

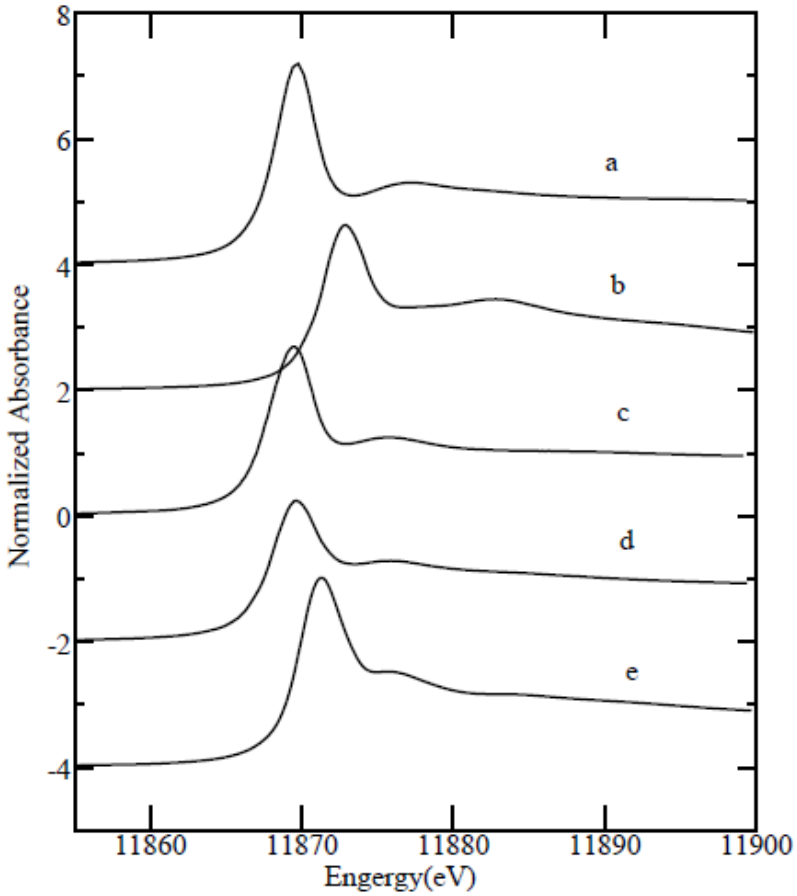

Figure 6.5 As K near-edge spectra of standard arsenic species.
a. $As(GS)_3$ (arsenic triglutathione)
b. $(CH_3)_3As{=}O$ (trimethylarsine oxide)
c. $[(GS)_2AsSe]^-$ (seleno-*bis*(S-glutathionyl) arsinium ion)
d. $CH_3As(HlipS_2)$ (a sulfur coordinated MMA^{III})
e. AsO_3^{3-} (arsenite)

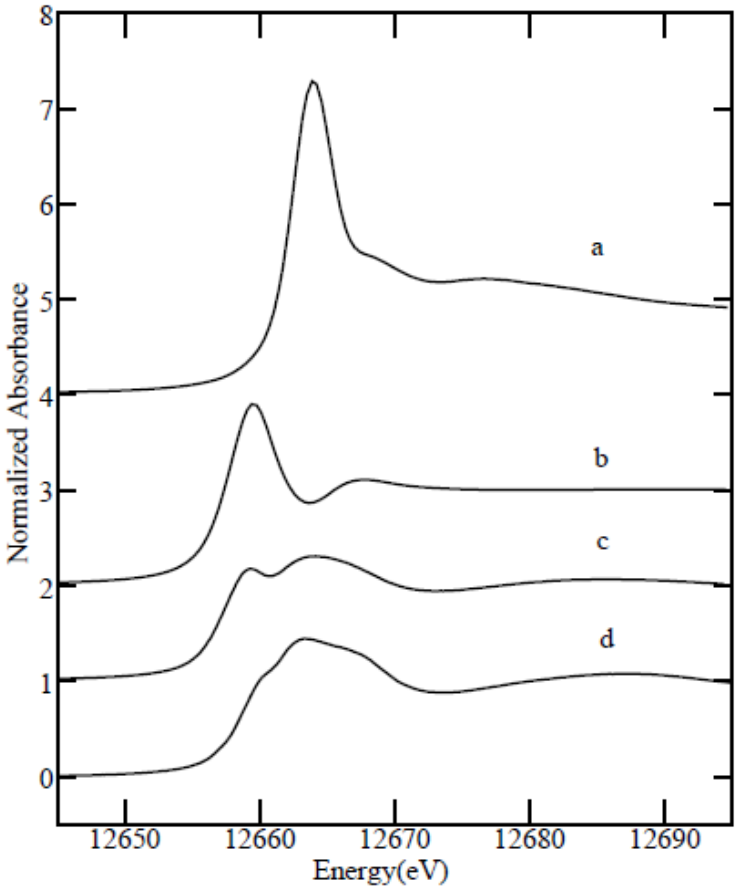

Figure 6.6 Selenium K near-edge spectra of standard selenium species.
a. SeO_3^{2-}(selenite)
b. α-Se (elemental selenium)
c. $[(GS)_2AsSe]^-$ (seleno-*bis*(S-glutathionyl) arsinium ion)
d. HSe^- (selenide)

6.2.1 Speciation of Arsenic and Selenium after Injection of Arsenite followed by Selenite

Both arsenic and selenium K near edge spectra were collected after injection of arsenite followed by selenite. Least squares fittings of the As and Se near-edge spectrum from red blood cell 5min post injection to the sum of spectra of the standard model species are shown in Figures 6.7 & 6.8. Whole blood, red blood cell and plasma samples from other time points were fitted using the same standard species; the summaries of the speciation results are shown in Tables 6.1 & 6.2.

These results indicate that the arsenite and selenite injected into blood forms $[(GS)_2AsSe]^-$, and some arsenic becomes methylated, forming species similar to $CH_3As(HlipS_2)$ and MMA^V. In red blood cells (Figure 6.1), $[(GS)_2AsSe]^-$ was found to be the most abundant arsenic species, with the fraction varying from 99% to 43%. $[(GS)_2AsSe]^-$ was the only arsenic species detected at 40min post injection of arsenite followed by selenite. At later time points in red blood cell, $CH_3As(HlipS_2)$ was also found, and the fractions of $CH_3As(HlipS_2)$ increased while the fractions of $[(GS)_2AsSe]^-$ decreased. This suggests that $[(GS)_2AsSe]^-$ was formed in red blood cell in agreement with earlier work (Gailer *et al.*, 2000). Plasma samples were fitted in the same manner and two components appear to yield the best fits to the data; $CH_3As(HlipS_2)$ and MMA^V. The concentrations of arsenic in plasma collected 5min post injection and later were low, resulting in small signals for the As K near-edge spectra with correspondingly poor signal

to noise. Because of this it is difficult to obtain accurate fractions for individual species; however, the data suggest that both $CH_3As(HlipS_2)$ and MMA^V are present.

A summary of selenium speciation results of whole blood, red blood cell and plasma samples after injection of arsenite followed by selenite is shown in Table 6.2. In whole blood and red blood cell samples, four components yield the best fits to the data; $[(GS)_2AsSe]^-$, HSe^-, α-Se and SeO_3^{2-}. HSe^- and α-Se were found to be the most abundant of all selenium species in whole blood and red blood cell samples within 2h post injection. Comparing all samples collected between 5min to 2h post injection, the 20min time point had the greatest fraction of $[(GS)_2AsSe]^-$ in whole blood and red blood cells. At later time points, the fractions of $[(GS)_2AsSe]^-$ decreased in whole blood and red blood cells. Also, more $[(GS)_2AsSe]^-$ was observed in red blood cell fractions compared with whole blood or plasma at each time point. No $[(GS)_2AsSe]^-$ species was detected in plasma samples with 2h post injection. Two components appeared to yield the best fits to the plasma data, α-Se and SeO_3^{2-}.

Figure 6.9 shows the kinetics of $[(GS)_2AsSe]^-$ in red blood cells 2h post injection of arsenite and then followed by selenite. The concentrations of $[(GS)_2AsSe]^-$ are derived from total Se/As concentration and Se/As speciation results. From figure 6.9, we can demonstrate that the kinetics of $[(GS)_2AsSe]^-$ in red blood cell after injection of arsenite and then followed by selenite is approximately first order. From figure 6.9, the half-life of $[(GS)_2AsSe]^-$ can be calculated as $t_{1/2}$=27.4min derived from selenium concentration (upper figure) and $t_{1/2}$=25.6min derived from arsenic concentration(lower figure). Given the various errors implicit in obtaining these values, they are in remarkable agreement.

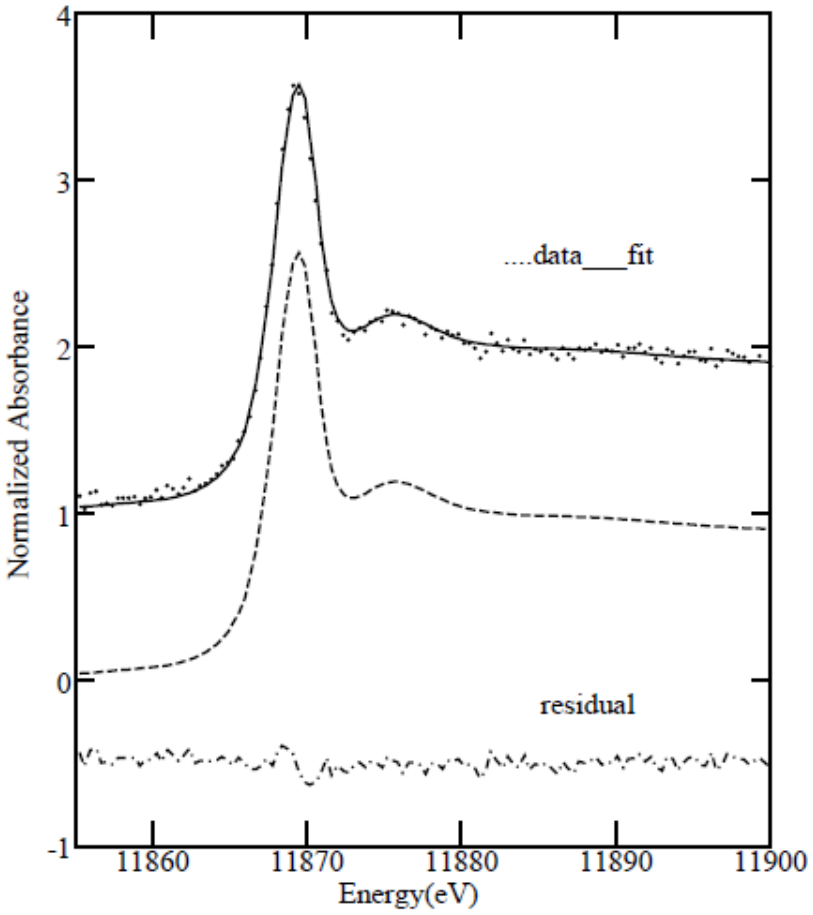

Figure 6.7 Least squares fit of the As K near-edge spectrum of red blood cell 5min post injection of arsenite followed by selenite to the sum of spectra of standard arsenic species. Shown are the red blood cell data (dotted line), the fit (solid line) and the individual component, scaled according to its contribution to the fit: $[(GS)_2AsSe]^-$. The residual is shown offset below. Numerical results are shown in Table 6.1.

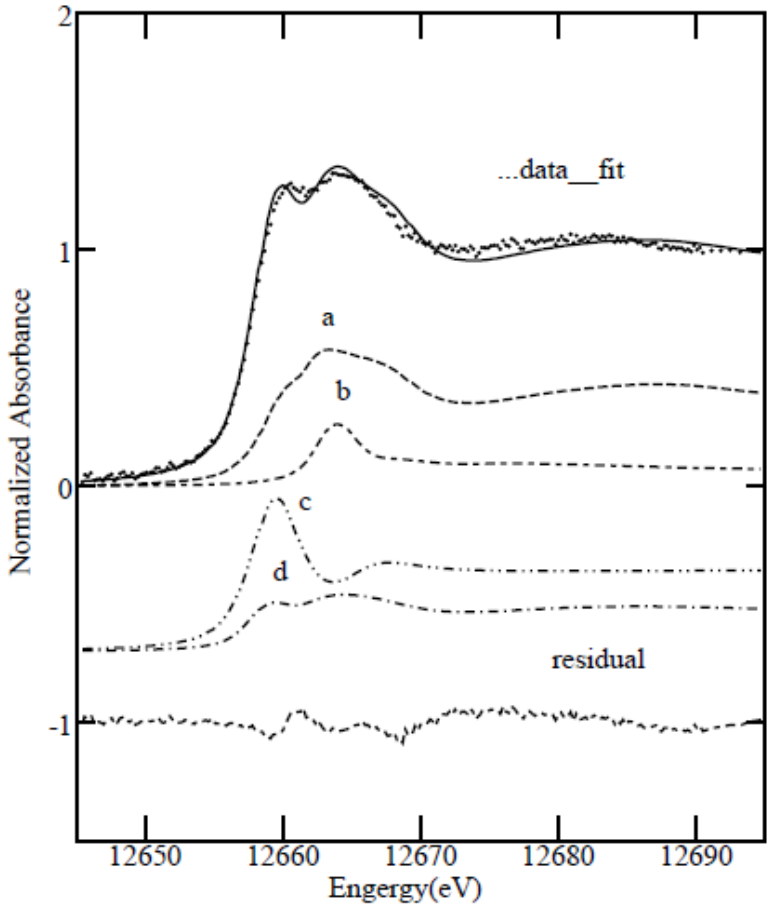

Figure 6.8 Least squares fit of the spectrum of rabbit red blood cell 5min after injection of arsenite followed by selenite to the sum of spectra of standard selenium species. Shown are the red blood cell data (dotted line), the fit (solid line) and the individual components, scaled according to their contributions to the fit: a. HSe^- b. SeO_3^{2-} c. α-Se d. $[(GS)_2AsSe]^-$ The residual is shown offset below. Numerical results are shown in Table 6.2.

Table 6.1 Percentage of arsenic as each arsenic species in rabbit blood samples after injection of arsenite followed by selenite.

Sample	**$[(GS)_2AsSe]^-$**	**$CH_3As(HlipS_2)$**	**MMA^V**
AsSe_w1_5min	86(12)	8(4)	6(3)
AsSe_w2_20min	73(8)	13(7)	14(6)
AsSe_w3_40min	48(9)	34(3)	18(5)
AsSe_w4_1hr	27(3)	54(8)	19(6)
AsSe_w5_2hr	22(3)	58(4)	20(3)
AsSe_R1_5min	100(1)	—	—
AsSe_R2_20min	100(3)	—	—
AsSe_R3_40min	100(3)	—	—
AsSe_R4_1hr	55(6)	45(9)	—
AsSe_R5_2hr	45(3)	55(4)	—
AsSe_PL1_5min*	—	78(13)	22(10)
AsSe_PL2_20min*	—	51(10)	49(8)

As K near-edge fitting results from whole blood (W), red blood cells (R) and plasma (PL) samples from the rabbit injected with arsenite followed by selenite, within 2h post injection. Values derived from percentage contributions of spectra of standards to the best fit of the sample spectra. Figures in parenthesis show three times standard deviation. Seleno-*bis*(S-glutathionyl) arsinium ion, (2-methyl-1,3,2-dithiarsinan-4-yl) pentanoic acid and dimethlyarsinic acid are represented by $[(GS)_2AsSe]^-$, $CH_3As(HlipS_2)$ and MMA^V, respectively. * indicates that sample is dilute resulting in poor data quality precluding accurate analysis, and only the major component is therefore determined.

Table 6.2 Percentage of selenium as each selenium species in rabbit blood samples after injection of arsenite followed by selenite.

Sample	**$[(GS)_2AsSe]^-$**	**HSe^-**	**α-Se**	**SeO_3^{2-}**
AsSe_w1_5min	8(1)	23(6)	54(3)	13(3)
AsSe_w2_20min	17(1)	14(5)	57(2)	12(2)
AsSe_w3_40min	9(1)	28(7)	52(3)	10(3)
AsSe_w4_1hr	5(1)	34(5)	51(2)	8(2)
AsSe_w5_2hr	4(1)	35(5)	50(3)	11(3)
AsSe_R1_5min	18(1)	40(5)	34(3)	8(2)
AsSe_R2_20min	41(1)	27(1)	26(2)	6(2)
AsSe_R3_40min	23(1)	37(2)	36(2)	3(1)
AsSe_R4_1hr	13(2)	40(7)	44(3)	6(3)
AsSe_R5_2hr	9(2)	34(5)	50(3)	6(2)
AsSe_PL1_5min	—	—	78(3)	20(3)
AsSe_PL2_20min	—	—	76(1)	24(1)
AsSe_PL3_40min	—	—	75(3)	27(3)
AsSe_PL4_1hr	—	—	74(2)	26(2)
AsSe_PL5_2hr	—	—	73(2)	26(2)

Edge fitting results of whole blood (W), red blood cells (R) and plasma (PL) samples from rabbit treated by arsenite followed by selenite, from 5mins after injection to 2hr after injection, respectively. Values derived from percentage contributions of spectra of standards to the best fit of the sample spectra. Figures in parenthesis show three times standard deviation. Seleno-bis (S-glutathionyl) arsinium ion, selenide, elemental selenium, selenite are represented by $[(GS)_2AsSe]^-$, HSe^-, α-Se and SeO_3^{2-}, respectively.

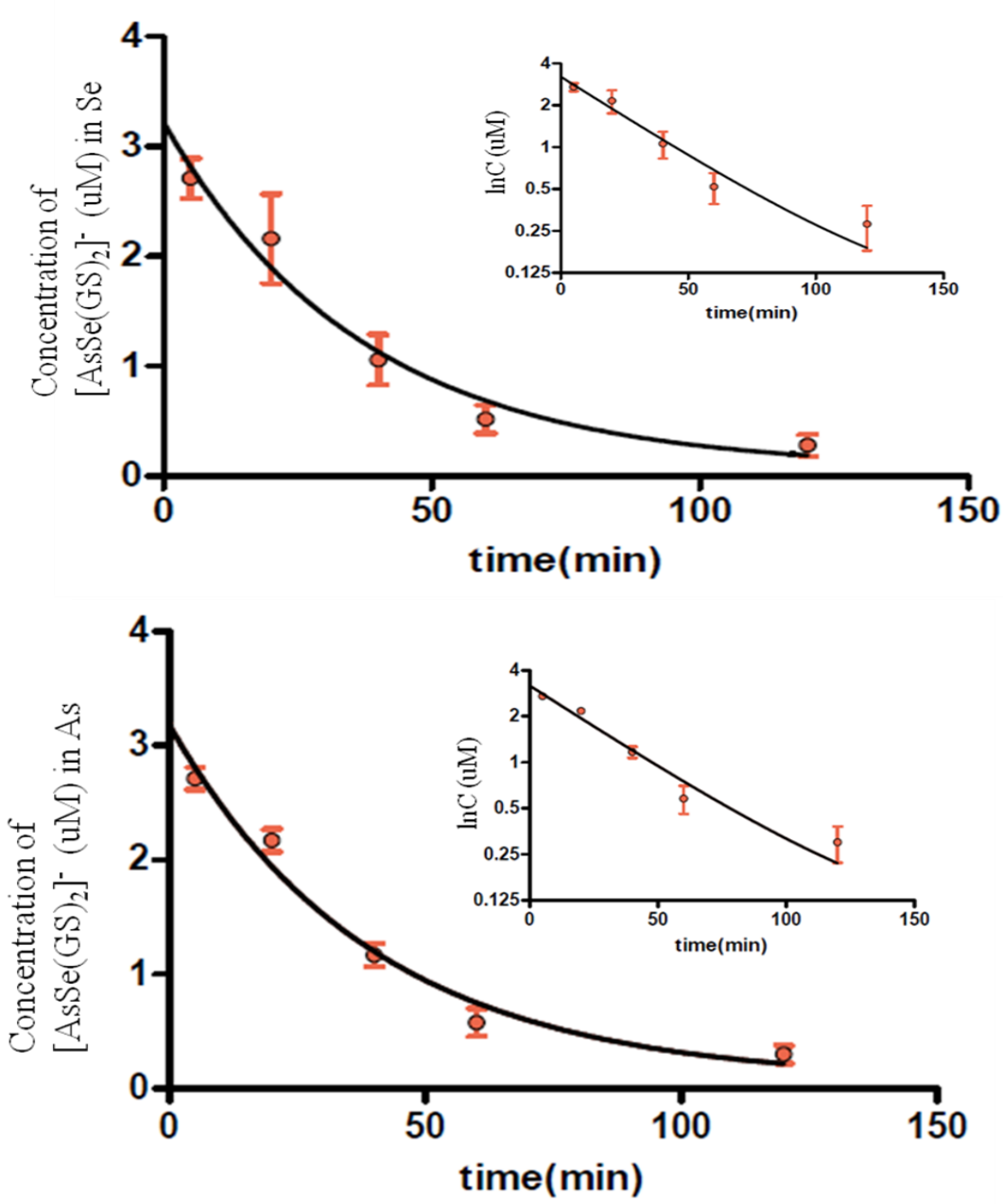

Figure 6.9 The concentrations of $[AsSe(GS)_2]^-$ in red blood cell samples vs. time within 2h post injection of arsenite followed by selenite derived from Se (upper) and As (lower) speciation results; inside figures show the semilog plots.

6.2.2 Speciation of Arsenic and Selenium after Injection of Selenite followed by Arsenite

Both arsenic and selenium K near-edge spectra of whole blood, red blood cells and plasma samples after injection of selenite followed by arsenite were collected. Figure 6.10 and Figure 6.11 show the variation of selenium and arsenic K near-edge spectra in whole blood, red blood cell and plasma spectra 5min post injection. The dotted vertical line helps emphasize the energy variation in the near edge spectra. Arsenic and Selenium near-edge spectra were fitted to the sum of spectra of the standard model species in Figure 6.5 and Figure 6.6.

.

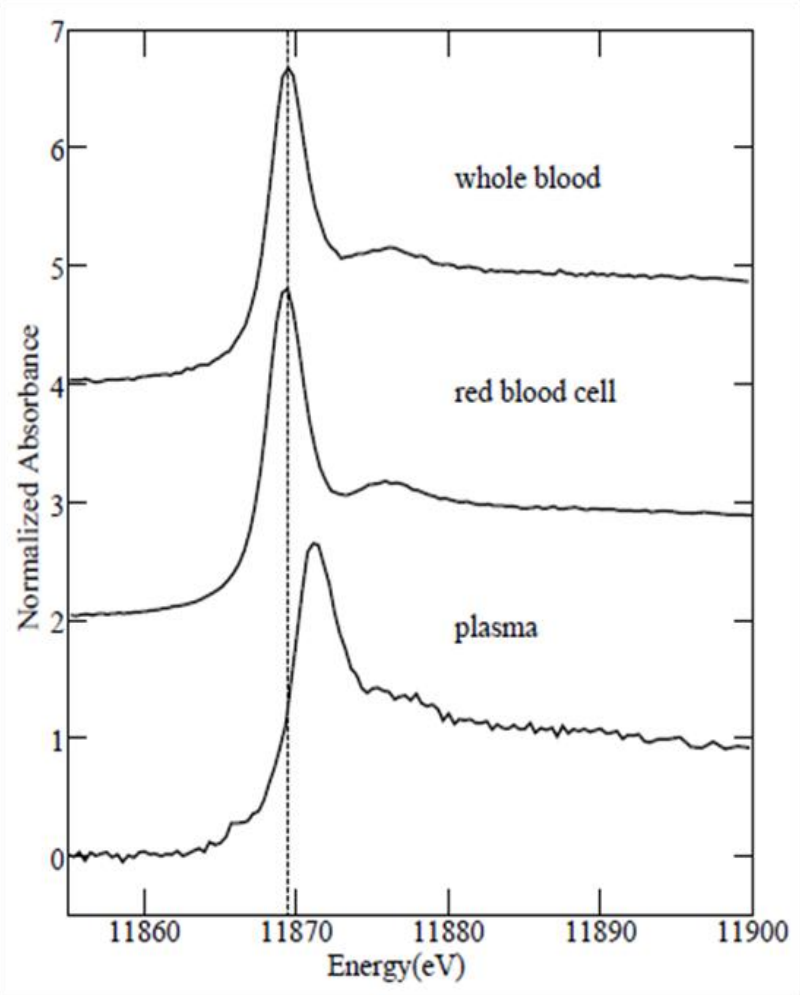

Figure 6.10 Arsenic K near-edge spectra of whole blood, red blood cell and plasma from the rabbit 5min after injection of selenite followed by arsenite. Dotted vertical line helps to emphasize the energy variation in the near edge.

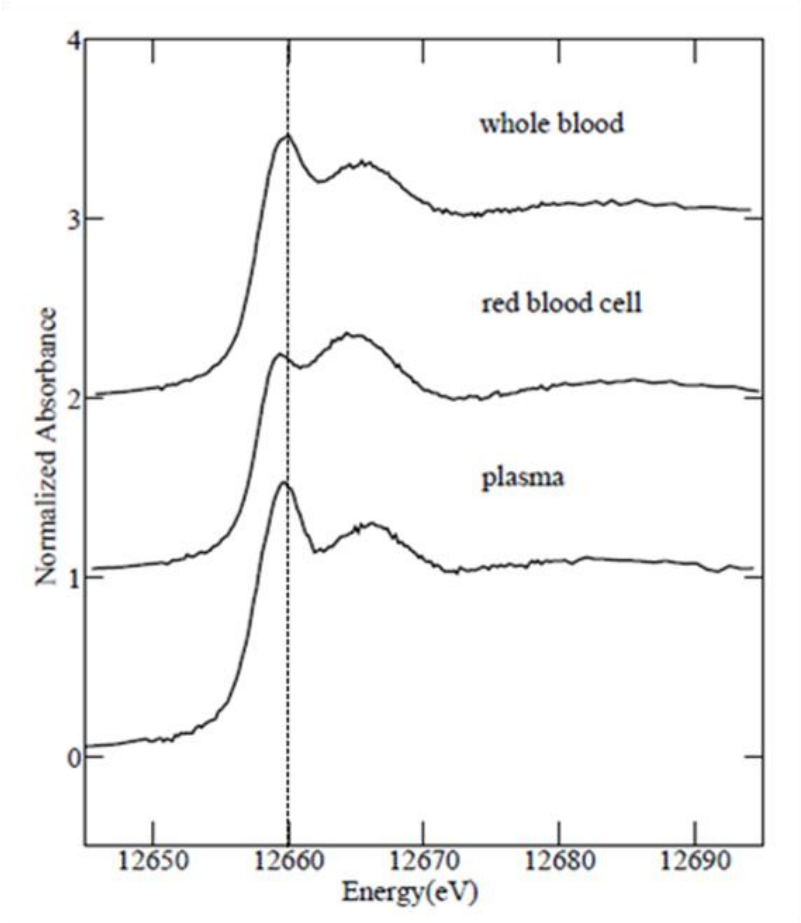

Figure 6.11 Selenium K near-edge spectra of whole blood, red blood cell and plasma from the rabbit 5min after injection of selenite followed by arsenite. The dotted vertical line helps to emphasize the energy variation in the near edge.

A summary of the arsenic speciation results after injection of selenite followed by arsenite is shown in Table 6.3. $[(GS)_2AsSe]^-$ was detected at 5min and 20min post injection in whole blood and red blood cell. At 5min time point, $[(GS)_2AsSe]^-$ had the highest fraction of 61% of total arsenic in whole blood and a fraction 72% in red blood cell. At 20min time point, $[(GS)_2AsSe]^-$ decreased to 7% of total arsenic in whole blood and 14% in red blood cell. At later time points, no significant amount of $[(GS)_2AsSe]^-$ was found in whole blood and red blood cell samples. No evidence of $[(GS)_2AsSe]^-$ was detected in plasma samples either. $CH_3As(HlipS_2)$ was found to be the most abundant of all arsenic species in whole blood within 2h post injection. $As(GS)_3$ was found in whole blood from 5min to 20min post injection, while it was present in red blood cell from 5min to 1h post injection. 20min after injection, $As(GS)_3$ was methylated to MMA^V and was largely cleared from whole blood. In red blood cell samples, $CH_3As(HlipS_2)$ and $As(GS)_3$ were the most abundant arsenic species 20min post injection. In plasma samples, arenite was found to be the most abundant of all arsenic species between 5min and 1h post injection, with this species comprising 91% to 26% of the total As content. $CH_3As(HlipS_2)$ and MMA^V were detected in plasma samples and the fraction of these arsenic species increased between 40min and 2h post injection.

A summary of the selenium speciation results after injection of selenite followed by arsenite is shown in Table 6.4. $[(GS)_2AsSe]^-$ was found 5min and 20min post injection in whole blood and red blood cell. At 5min time point, $[(GS)_2AsSe]^-$ had the highest fraction of 20% of total selenium in whole blood and a fraction 35% in red blood cell. At

20min time point, $[(GS)_2AsSe]^-$ decreased to 5% of total selenium in whole blood and 8% in red blood cell. At later time points, no significant amount of $[(GS)_2AsSe]^-$ was found in whole blood and red blood cell samples. No evidence of $[(GS)_2AsSe]^-$ was detected in plasma samples either. Across all time points studied, HSe^- and α-Se were found to be the most abundant of all selenium species, with HSe^- comprising 35% to 66% of the total selenium content; while the fraction of α-Se varying from 29% to 65% of the total selenium content in whole blood, red blood cell and plasma. From 5min to 20min post injection, the fraction of 3% to 4% of selenite was also been detected in whole blood and red blood cell.

Table 6.3 Percentage of arsenic as each arsenic species in rabbit blood samples after injection of selenite followed by arsenite.

Sample	**$[(GS)_2AsSe]^-$**	**AsO_3^{3-}**	**$CH_3As(HlipS_2)$**	**$As(GS)_3$**	**MMA^V**
SeAs_w1_5min	61(6)	—	4(2)	37(6)	—
SeAs_w2_20min	7(3)	—	81(5)	11(2)	—
SeAs_w3_40min	—	—	95(3)	—	5(2)
SeAs_w4_1hr	—	—	86(5)	—	15(3)
SeAs_w5_2hr	—	—	75(7)	—	25(4)
SeAs_R1_5min	72 (6)	—	—	27(6)	—
SeAs_R2_20min	14(8)	—	24(5)	62(7)	—
SeAs_R3_40min	—	—	46(8)	53(5)	—
SeAs_R4_1hr	—	—	55(6)	45(4)	—
SeAs_R5_2hr	—	—	85(6)	—	15(5)
SeAs_PL1_5min	—	91(4)	7(2)	—	—
SeAs_PL2_20min	—	88(7)	12(8)	—	—
SeAs_PL3_40min	—	63(8)	—	13(7)	23(4)
SeAs_PL4_1hr	—	26(6)	—	27(7)	47(5)
SeAs_PL5_2hr	—	—	—	38(9)	62(9)

As K near-edge fitting results from whole blood (W), red blood cells (R) and plasma (PL) samples from the rabbit injected with selenite followed by arsenite, within 2h post injection. Values derived from percentage contributions of spectra of standards to the best fit of the sample spectra. Figures in parenthesis show three times standard deviation. Seleno-*bis*(S-glutathionyl) arsinium ion, arsenite, tri-glutathione arsenic, (2-methyl-1,3,2-dithiarsinan-4-yl) pentanoic acid and monomethylarsonic acid are represented by $[(GS)_2AsSe]^-$, AsO_3^{3-}, $As(GS)_3$, $CH_3As(HlipS_2)$ and MMA^V, respectively.

Table 6.4 Percentage of selenium as each selenium species in rabbit blood samples after injection of selenite followed by arsenite.

Sample	**$[(GS)_2AsSe]^-$**	**HSe^-**	**α-Se**	**SeO_3^{2-}**
SeAs_w1_5min	20(2)	31(3)	45(2)	4(2)
SeAs_w2_20min	5(1)	36(4)	55(2)	3(1)
SeAs_w3_40min	—	55(5)	45(5)	—
SeAs_w4_1hr	—	55(5)	45(5)	—
SeAs_w5_2hr	—	60(6)	40(5)	—
SeAs_R1_5min	35(2)	32(4)	29(3)	4(2)
SeAs_R2_20min	8(2)	48(3)	40(3)	3(2)
SeAs_R3_40min	—	67(4)	33(3)	—
SeAs_R4_1hr	—	66(4)	34(3)	—
SeAs_R5_2hr	—	66(4)	34(6)	—
SeAs_PL1_5min	—	35(6)	65(3)	—
SeAs_PL2_20min	—	42(3)	58(3)	—
SeAs_PL3_40min	—	42(10)	58(5)	—
SeAs_PL4_1hr	—	55(5)	45(5)	—
SeAs_PL5_2hr	—	49(5)	51(5)	—

Edge fitting results of whole blood (W), red blood cells (R) and plasma (PL) samples from rabbit treated by selenite followed by arsenite, from 5mins after injection to 2hr after injection, respectively. Values derived from percentage contributions of spectra of standards to the best fit of the sample spectra. Figures in parenthesis show three times standard deviation. Seleno-bis (S-glutathionyl) arsinium ion, selenide, elemental selenium and selenite are represented by $[(GS)_2AsSe]^-$, HSe^-, α-Se and SeO_3^{2-}, respectively.

6.3 Speciation of Arsenic in Cecotrope after Injection of Arsenite and Selenite

The spectra of cecotrope samples 24h post injection of both arsenite and selenite were also collected. Least squares fits of spectra of cecotrope sample after injection of selenite followed by arsenite to the sum of spectra of standard species are shown in Figure 6.12 & 6.13. Cecotrope sample after injection of arsenite followed by selenite was fitted to the standard selenium and arsenic species of in the same manner; the results of which are shown in Tables 6.5 & 6.6.

The samples were random picked up from a pool of cecotrope samples the rabbit produced over night, and the experimental results were primary since it is hard to detect when exactly the cecotrope samples were produced post injection. From Table 6.5, $[(GS)_2AsSe]^-$ was detected in both ceocotrope samples regardless of the order of the injection of arsenite and selenite. Cecotrope sample collected from the rabbit which was injected arsenite first, had a fraction of 78% of $[(GS)_2AsSe]^-$ and the other arsenic species found was arsenite. A fraction of 45% of $(CH_3)_3As{=}O$ was found in the cecotrope sample from the rabbit which was injected by selenite first. It is still unclear why $(CH_3)_3As{=}O$ is formed but one possible guess is $(CH_3)_3As{=}O$ is the metabolite of some bacteria from the gut of the rabbit.

Table 6.6 shows the least square fitting results of selenium spectra of cecotrope samples. There were four components in selenium speciation of both cecotrope samples,

$[(GS)_2AsSe]^-$, SeO_3^{2-},GS-Se-GS and R-Se-R. Among of the four components, GS-Se-GS had the greatest fraction at around 50% of the total selenium content, and $[(GS)_2AsSe]^-$ had the second greatest fraction as well as selenite had the smallest fraction.

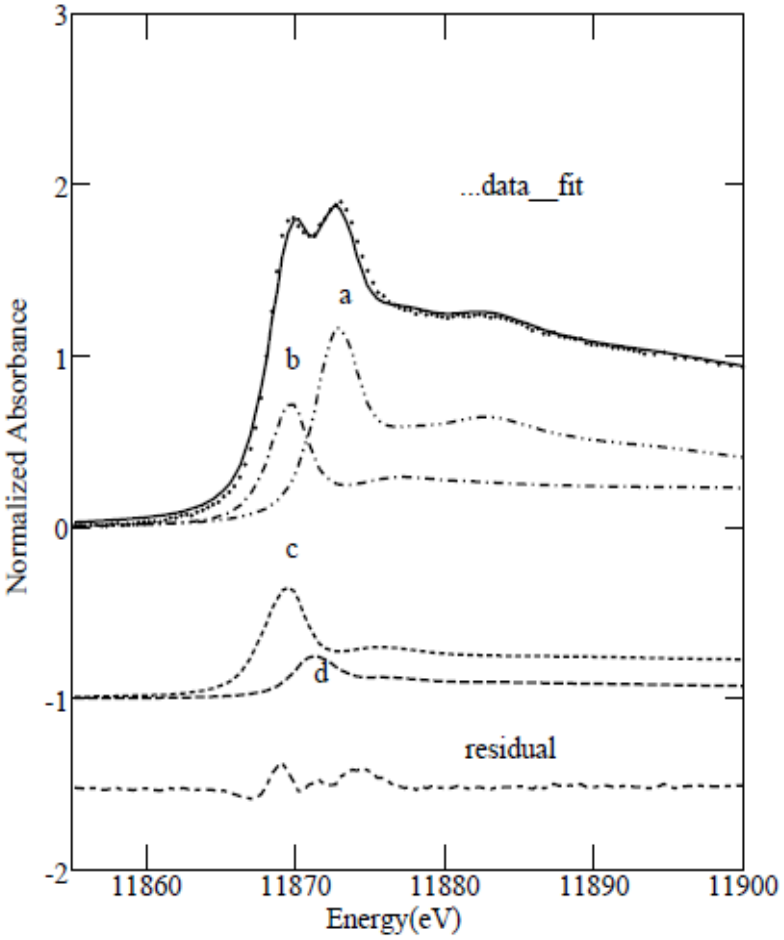

Figure 6.12 Least squares fit of the As K-edge spectrum of cecotrope from a rabbit 24 hours after injection by selenite followed by arsenite. The spectrum was fitted to the sum of spectra of model species. Figure shows the cecotrope data (dotted line), the fit (black line) and the individual components, scaled according to their contributions to the fit.

a. $(CH_3)_3As=O$ b. $[(GS)_2AsSe]^-$ c. $As(GS)_3$ d. arsenite

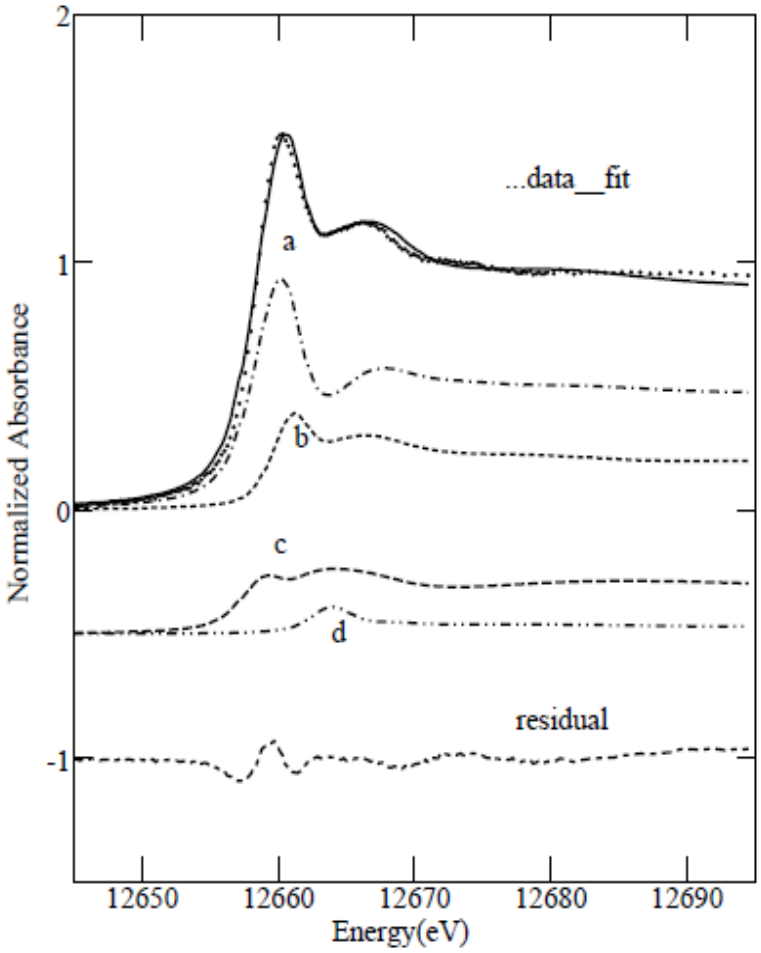

Figure 6.13 Least squares fit of the Se K-edge spectrum of cecotrope from a rabbit 24 hours after injection by selenite followed by arsenite. The spectrum was fitted to the sum of spectra of model species. Figure shows the cecotrope data (dotted line), the fit (black line) and the individual components, scaled according to their contributions to the fit.

a. GS-Se-GS b. R-Se-R c. $[(GS)_2AsSe]^-$ d. SeO_3^{2-}

Table 6.5 Percentage of arsenic as each arsenic species in rabbit cecotrope samples after injection of arsenite and selenite, either in this order (SeAs) or reversed (AsSe).

Sample	**$[(GS)_2AsSe]^-$**	**$CH_3As(HlipS_2)$**	**AsO_3^{3-}**	**$As(GS)_3$**	**$(CH_3)_3As=O$**
SeAs	24(9)	—	8(3)	23(9)	45(3)
AsSe	71(2)	29(3)	—	—	—

Edge fitting results of cecotrope sample from rabbit injected by selenite followed by arsenite (SeAs) and cecotrope sample from rabbit injected arsenite followed by selenite (AsSe). Values derived from percentage contributions of spectra of standards to the best fit of the sample spectra. Figures in parenthesis show three times standard deviation. Seleno-*bis*(S-glutathionyl) arsinium ion, sulfur coordinated MMA^{III}, arsenite, arsenic tri-glutathione and trimethylarsine oxide are represented by $[(GS)_2AsSe]^-$, $CH_3As(HlipS_2)$, AsO_3^{3-} , $As(GS)_3$and $(CH_3)_3As=O$, respectively.

Table 6.6 Percentage of selenium as each selenium species in rabbit cecotrope samples after injection of arsenite and selenite, either in this order (SeAs) or reversed (AsSe).

Sample	**$[(GS)_2AsSe]^-$**	**SeO_3^{2-}**	**GS-Se-GS**	**R-Se-R**
SeAs	22(6)	3(2)	53(6)	23(5)
AsSe	37(7)	8(3)	47(7)	13(5)

Edge fitting results of cecotrope sample from rabbit injected by selenite followed by arsenite (SeAs) and cecotrope sample from rabbit injected arsenite followed by selenite (AsSe). Values derived from percentage contributions of spectra of standards to the best fit of the sample spectra. Figures in parenthesis show three times standard deviation. Seleno-*bis*(S-glutathionyl) arsinium ion, selenite, selenodiglutathione and selenomethionineare represented by $[(GS)_2AsSe]^-$, SeO_3^{2-},GS-Se-GS and R-Se-R, respectively.

6.4 Discussion

The results above show that after injection of both selenite and arsenite into rabbit, regardless of the order of injection, blood arsenic accumulates in red blood cells as opposed to plasma; $[(GS)_2AsSe]^-$ was found in red blood cell 5min post injection but not in plasma. This indicates that $[(GS)_2AsSe]^-$ is assembled in red blood cell and is formed in blood very rapidly. Earlier studies have also shown similar results (Gailer *et al.*, 2000)

When arsenite was injected into rabbit before selenite, $[(GS)_2AsSe]^-$ was detected in red blood cell at 100% of total arsenic in blood between 5min and 40min post injection. $[(GS)_2AsSe]^-$ started to eliminate from blood 1h post injection, and $CH_3As(HlipS_2)$ was the main metabolite in red blood cell within 2hrs after injection. The arsenic in plasma fractions presented as the methylated species similar to $CH_3As(HlipS_2)$ and MMA^V. Our experimental results demonstrate that 71% of total arsenic in the form of $[(GS)_2AsSe]^-$ is one of the end products of arsenic in cecotrope sample after injection.

When arsenite was injected into rabbit after selenite, $[(GS)_2AsSe]^-$ was found in red blood cell 5min and 20min post injection at a fraction of 72% and 14%, respectively. At 40min post injection, $[(GS)_2AsSe]^-$ was not detected in blood which indicates $[(GS)_2AsSe]^-$ had been largely removed from blood stream. Although $[(GS)_2AsSe]^-$ was first found at 5min time point, it is very likely that $[(GS)_2AsSe]^-$ would be detected in red blood cell before 5min at a fraction higher than 72% of total arsenic. Based on our experiment results, one possible guess is that $[(GS)_2AsSe]^-$ is formed in red blood cell as the moment arsenic and selenium meet in blood and then start to be removed from blood

within 40min. 40min post injection, $[(GS)_2AsSe]^-$ had been removed from blood and thus $CH_3As(HlipS_2)$ and MMA^V were found to be the main metabolites of arsenic in blood. 24hr after injection, $[(GS)_2AsSe]^-$ had also been detected in cecotrope sample.

In conclusion, when administration arsenite and selenite into rabbit, the nontoxic species of $[(GS)_2AsSe]^-$ will be formed in red blood cell very rapidly and then start to be removed from blood system within 40min post injection.

Chapter 7: General Discussion and Future Work

7.1 The Behaviour of Arsenic in the Absence and Presence of Selenium

In this study, X-ray absorption spectroscopy was used to investigate the molecular-level disposition of arsenic and selenium in rabbit upon the treatment of selenite, arsenite or both. Whole blood, red blood cell, plasma and cecotrope samples were examined in this study. In the absence and presence of selenium, arsenic behaves very differently. In the absence of selenium, arsenic rapidly accumulates in red blood cells as opposed to plasma. In our experiments, the end product of arsenic in blood was found to be related to the mono-methylated model $CH_3As(HlipS_2)$ which contains arsenic coordinated by two thiolates and a single methyl group 2h post injection of arsenite to the rabbit. In addition, species resembling $CH_3As(HlipS_2)$ were also detected in cecotrope samples at a fraction of 84% of total arsenic content 24h post injection. The finding of $As(GS)_3$ species in blood after injection of arsenite supports the hypothesis that $As(GS)_3$ is an intermediate during arsenic biotransformation in the metabolic pathway for inorganic arsenic (Hayakawa *et al*., 2005). Hayakawa also suggested that the end products of arsenic metabolism are MMA(III) and DMA(III). However, in our experiments, no evidence of those methylated species was found, although it is possible that they might be found in urine.

In the presence of selenium, when rabbit was injected with selenite followed by arsenite, $As(GS)_3$ and $CH_3As(HlipS_2)$ were detected in red blood cells and plasma samples within 2hr post injection, which also suggesting that the transformation from $As(GS)_3$ to $CH_3As(HlipS_2)$ was in process during arsenic metabolism. However, when rabbit was injected with arsenite followed by selenite, $As(GS)_3$ cannot be detected in blood samples but $CH_3As(HlipS_2)$ was still found. It is possible that the transformation from $As(GS)_3$ to $CH_3As(HlipS_2)$ was too fast to detect. Regardless of the order of injection, MMA^V was found to be the end product after injection of arenite and selenite.

When selenite and arsenite were given together into the rabbit, regardless of the order of the injections, the complex -- $[(GS)_2AsSe]^-$ was formed in red blood cell very rapidly (within 5mins post injection). Our experimental results demonstrated that 99%±1% of total arsenic detected in blood appears in the form of $[(GS)_2AsSe]^-$ at the shortest time measured. 40min after injection, $[(GS)_2AsSe]^-$ had largely been eliminated from blood. This shows that $[(GS)_2AsSe]^-$ was removed from red blood cells. Researchers in Alberta reported that *in vitro* red blood cells don't transport $[(GS)_2AsSe]^-$ but did not use plasma (Carew and Leslie, 2010). However, our experimental results indicate that *in vivo*, red blood cells probably do transport $[(GS)_2AsSe]^-$. Although it is uncertain how $[(GS)_2AsSe]^-$ gets out from red blood cells, it is likely that some sort of ATP-driven transportation is involved. Also, compared to selenium, the elimination rate of arsenic in blood was higher. When arsenite was injected into rabbit after selenite, $[(GS)_2AsSe]^-$ could not be detected in blood 40min post injection, but it was found in the

blood system 2hr post injection when the dose was given in reverse. This indicated that $[(GS)_2AsSe]^-$ was eliminated from the blood faster when selenite was injected to the rabbit prior to arsenite. These findings suggested that the presence of selenite present in the system speeds up the removal of arsenic from the blood. Our experimental results also indicate that in rabbit injected selenium would deplete the body load of arsenic and toxic inorganic arsenic can be converted into the excretale species of $[(GS)_2AsSe]^-$.

It is very important to understand the metabolism of $[(GS)_2AsSe]^-$ and its excretion pathways. In addition to examine the cecotrope samples collected after injection of both arsenite and selenite, feces samples were collected and examined on the beamline. No significant amount of arsenic was detected. Due to the limitation of beamtime availability and the experimental loads, only blood and cecotrope samples were examined in this thesis. However, urine and bile samples are strongly suggested to be tested in the future work.

Eextrapolating from our rabbit results, the formation of $[(GS)_2AsSe]^-$ in blood should also consume the body load of arsenic in humans. Therefore, administering selenium supplements might provide a simple but highly effective treatment of Bangladeshi people who are suffering from long-term chronic low-level arsenic poisoning.

7.2 Future Work

The studies described in this thesis provide important information on the biochemistry of arsenic and selenium. In future work, the fate of arsenite and selenite following oral administration could be studied. Blood and cecotrope samples should be collected at different time intervals. Due to individual and bioavailability differences in different rabbits, various doses of arsenite and selenite should be tested to the rabbits. Both arsenic and selenium K near-edge spectra need to be recorded and analyzed for quantities and speciation studies. These results will give us a better idea of how fast $[(GS)_2AsSe]^-$ is formed in blood sample when arsenite and selenite is taken orally and how fast it is removed from blood. Urine and bile samples at different time intervals after injection should also be collected. Examination of urine and bile samples will indicate how $[(GS)_2AsSe]^-$ would be cleared from the body other than excreted in cecotropes.

References

Antman, K. H. (2001) "The History of Arsenic Trioxide in Cancer Therapy". *The oncologist*, **6**: 1–2.

Aposhian, H. V., and Aposhian, M. M. (2006) "Arsenic toxicology: five questions". *Chemical Research in Toxicology*, **19**: 1-15.

Aposhian, H. V., Zheng, B., Aposhian, M. M., Le, X. C., Cebrian, M. E., Cullen, W., Zakharyan, R. A., Ma, M., Dart, R. C., Cheng, Z., et al. (2000) "DMPS-arsenic challenge test. II. Modulation of arsenic species, including monomethylarsonous acid (MMA^{III}), excreted in human urine". *Toxicology and Applied Pharmacology*, **165**: 74–83.

Baum, M.K., Shor-Posner, G., Lai, S., Zhang, G., Lai, H., Fletcher, L.A., Sauberlich, H., Page, J.B. (1997) "High risk of HIV-related mortality is associated with selenium deficiency". *Journal of Acquired Immune Deficiency Syndromes and Human Retrovirology*, **15**: 370–4.

Berzelius, J. J. (1818) "Lettre de M. Berzelius à M. Berthollet sur deux métaux nouveaux" (Letter from Mr. Berzelius to Mr. Berthollet on two new metals), *Annales de chimie et de physique*, **2**: 199-206.

Bleys, J., Navas-Acien, A., and Guallar, E. (2007) "Serum selenium and diabetes in U.S. adults". *Diabetes Care*, **30**: 829–34.

Breslow, E.L., and Cengage, G. (2002) "Arsenic". *Encyclopedia of Public Health.* <http://www.enotes.com/public-health-encyclopedia/arsenic>

Burk, R. F., Hill, K. E. (2009) "Selenoprotein P-Expression, functions, and roles in mammals". *Biochimica et Biophysica Acta, General Subjects*, **1790**: 1441-1447.

Caravati, E.M. (2004) “Arsenic and arsenic gas”. In Dart, R.C. and Carabati, E.M.(eds) *Medical toxicology,*1393–1401, Philadelphia, Lippincott Williams & Wilkins.

Carew, M. W., and Leslie, E. M. (2010) “Selenium-dependent and -independent transport of arsenic by the human multidrug resistance protein 2 (MRP2/ABCC2): implications for the mutual detoxification of arsenic and selenium”. *Carcinogenesis,* **31**: 1450-1455.

Carter, D. E., Aposhian, H. V., and Gandolfi, A. J. (2003) “The metabolism of inorganic arsenic oxides, gallium arsenide, and arsine: A toxicochemical review”. *Toxicology and Applied Pharmacology,* **193**: 309-334.

Chaudhuri, A. (2004) “Dealing with arsenic contamination in Bangladesh”. *MIT Undergrad Research Journal,* **11**: 25–30.

Chen, X., Y, G., Chen, J., Chen, X., Wen, X., and Ge, K. (1980) “Studies on the relations of selenium and Keshan disease”. *Biological Trace Element Research,* **2**:91-107.

CLS (Canadian Light Source Inc) (2010) “Canadian Light Source Virtual Tour”. <http://www.lightsource.ca/education/vr.php>

Cuvin-Aralar, M.L., and Furness, R.W. (1991) Mercury and selenium interaction: a review. *Ecotoxicology and Environmental Safet*y, **21**:348-64.

Du Bois, K.P., Moxon, A. L., and Olson, O.E. (1940) “Further studies on the effectiveness of arsenic in preventing selenium poisoning”. *Journal of Nutrition,* **19**:477.

Elder, F. R., Gurewitsch, A. M., Langmuir, R. V., and Pollock, H. C. (1947) “Radiation from Electrons in a Synchrotron”. *Physical Review,* **71**:829-830.

Emsley, John. (2001) “Nature's Building Blocks: An A-Z Guide to the Elements”. 40-45, Oxford, New York, Oxford University Press.

Gailer, J., George, G. N., Pickering, I.J., Prince, R. C., Ringwald, S. C., Pemberton, J. E., Glass, R. S., Younis, H. S., Deyoung, D. W., and Aposhian, H. V. (2000) “A metabolic link between arsenite and selenite: The Seleno-bis(S-glutathionyl) Arsinium Ion”. *Journal of the American Chemical Society*, **122**: 4637-4639

Gailer, J., George, G.N., Pickering, I.J., Madden, S, Prince, R.C., Yu, E.Y., Denton, M.B., Younis H.S., and Aposhian, H.V. (2000) “The Structural Basis of the Antagonism between Inorganic Mercury and Selenium in Mammals”. *Chemical Research in Toxicology,* **13**: 1135-1142.

Gailer, J., Madden, S., Burke, M. F., Denton, M. B., and Aposhian, H. V. (2000) “Simultaneous multielement-specific detection of a novel glutathione-arsenic-selenium ion $[(GS)_2AsSe]^-$ by ICP-AES after micellar size-exclusion chromatography”. *Applied Organometallic Chemistry*, **14**: 355-363.

Gailer, J., Ruprecht, L., Reitmeir, P., Benker, B., and Schramel, P. (2004) “Mobilization of exogenous and endogenous selenium to bile after the intravenous administration of environmentally relevant doses of arsenite to rabbits”. *Applied Organometallic Chemistry,* **18** : 670-675.

George, G.N. (2010) “Speciation of Mixtures”. <http://www-conf.slac.stanford.edu/smbxas-ss/2010/talks/George_06.pdf>

George, G.N. and Pickering, I.J. (2007) “X-ray Absorption Spectroscopy in Biology and Chemistry”. In Vasili Tsakanov and Helmut Wiedemann (eds), *Brilliant Light in Life and Material Sciences*, 97-119, New York, Springer.

George, G.N., and Pickering, I.J. (2000) EXAFSPAK. <http://www-ssrl.slac.stanford.edu/~george/exafspak/manual.pdf>

Gomez-Caminero, A., Howe, P., Hughes, M., Kenyon, E., Lewis, D.R., Moore, M., Ng, J., and Aitio, A., and Becking, G. (2001) "Arsenic and Arsenic Compounds", *Environmental Health Criteria* 224, 1-3, Genera, World Health Organization.

Gonsebatt, M.E., Vega, L., Salazar, A.M., Montero, R., Guzman, P., Blas, J., Del Razo, L.M., Garcia-Vargas, G., Albores, A., Cebrian, M.E., Kelsh, M., and Ostrosky-Wegman, P. (1997) "Cytogenetic effects in human exposure to arsenic". *Mutation Research*, **386**: 219–228.

Goyens P., Golstein J., Nsombola B., Vis H. and Dumont J. E. (1987) "Selenium deficiency as a possible factor in the pathogenesis of myxoedematous endemic cretinism". *Acta Endocrinologica,* **114**: 497-502.

Guha Mazumder, D.N. (2008) "Chronic arsenic toxicity & human health". *Indian Journal of medical research*, **28**:436-447.

Hayakawa, T., Kobayashi, Y., Cui, X., and Hirano, S. (2005) "A new metabolic pathway of arsenite: Arsenic-glutathione complexes are substrates for human arsenic methyltransferase Cyt19". *Achieves of Toxicology*, **79**: 183–191.

Hirakawa, H. (2001) "Coprophagy in Leporids and Other Mammalian Herbivores". *Mammal Review,* **31**: 61–80.

House, J. E. (2008) "Inorganic chemistry", 524, London, Academic Press.

Huerga, A., Lavilla, I., and Bendicho, C. (2005) "Speciation of the immediately mobilisable As(III), As(V), MMA and DMA in river sediments by high performance

liquid chromatography–hydride generation–atomic fluorescence spectrometry following ultrasonic extraction". *Analytica Chimica Acta,* **534**: 121-128.

Hughes, M.F. (2002) "Arsenic toxicity and potential mechanisms of action." *Toxicology letters*, **133**: 1-6.

Hutchinson, J. (1987) "Arsenic and cancer". *British Medical Journal,* **2**: 1280–1281

Institute of Medicine, Food and Nutrition Board. (2000) "Dietary Reference Intakes: Vitamin C, Vitamin E, Selenium, and Carotenoids". Washington, DC, National Academy Press.

Jones, D.P., Carlson, J.L., Mody, V.C., Cai, J., Lynn, M.J., and Sternberg, P. (2000) "Redox state of glutathione in human plasma". *Free Radical Biology & Medicine*, **28**:625-635.

Kudo, K. (1965) "Optical Properties of Plane-Grating Monochromator". *Journal of the Optical Society of America*, **55**: 150-161

Leng, L., Bobček, R., Kuricova, S., Boldizarova, K., Grešakova, L., Ševcikova, Z., Revajova, V., Levkutova, M., and Levkut, M. (2003) "Comparative metabolic and immune responses of chickens fed diets containing inorganic selenium and Sel-PlexTM organic selenium". In Lyons T.P., Jacques K.A. (eds.), *Nutritional Biotechnology in the Feed and Food Industries*, 131–145. Nottingham, U.K., Nottingham University Press.

Levander, O. A. (1977) "Metabolic interrelationships between arsenic and selenium". *Environmental Health Perspectives*, **19**:159-164

Lu, M., Wang, H., Li, X. F., Lu, X., Cullen, W. R., Arnold, L. L., Cohen, S. M., and Le, X. C. (2004) "Evidence of hemoglobin binding to arsenic as a basis for the accumulation of arsenic in rat blood". *Chemical Research in Toxicology,* **17**: 1733-1742.

Mäki-Paakkanen, J., Kurttio P., Paldy, A., and Pekkanen, J. (1998) "Association between the clastogenic effect in peripheral lymphocytes and human exposure to arsenic through drinking water". *Environmental and Molecular Mutagenesis,* **32**: 301–13.

Männistö, S., Alfthan, G., Virtanen, M., Kataja, V., Uusitupa, M., and Pietinen, P. (2000) "Toenail selenium and breast cancer ---a case-control study in Finland", *European Journal of Clinical Nutrition,* **54**: 98-103.

Masters, A. F. (2009) "Allotropes - Group 13, Group 14, Group 15, Group 16". *Chemistry Explained*. http://www.chemistryexplained.com/A-Ar/Allotropes.html

Moreno-Reyes, R., Suetens, C., Mathieu, F., Begaux, F., Zhu, D., Rivera, M.T., Boelaert, M., Neve, J., Perlmutter, N., and Vanderpas, J. (1998) "Kashin-Beck osteoarthropathy in rural Tibet in relation to selenium and iodine status". *The New England Journal of Medicine,* **339**: 1112–20.

Mortoza, S. (1997) "Arsenic contamination: searching for solutions-1997". <http://bicn.com/acic/resources/infobank/mortoza/mortoza1.htm>

Moxon, A.L. (1938) "The Effect of Arsenic on the Toxicity of Seleniferous Grains". *Science,* **88**:81–81

NTP, (National Toxicology Program), (2000). "Arsenic and certain arsenic compounds". *Reports on Carcinogens, First and Subsequent 2nd–9th (1980–2000),* 17–19. Research Triangle Park, NC.

Patrick, L. (1999) “Nutrients and HIV: part one ─ beta carotene and selenium”. *Alternative Medicine Review*, **4**: 403–13

Petrick, J. S., Ayala-Fierro, F., Cullen, W. R., Carter, D. E., and Aposhian, H. V. (2000) “Monomethylarsonous acid MMA(III) is more toxic than arsenite in Chang human hepatocytes”. *Toxicology and Applied Pharmacology*, **163**: 203-207.

Petrusevski, B., Sharma, S.K., and Schippers, J.C. (2005) Arsenic in drinking water (Part I). *Voda i Sanitarna Technika*, **35**: 11-18.

Pickering, I.J., Prince, R.C., Divers, T., and George, G.N. (1998) “Sulfur K-edge X-ray Absorption spectroscopy for determining the chemical speciation of sulfur in biological systems”. *FEBS Letters*, **441**:11-14.

Rahman, F.A., Allan, D.L., Rosen, C.J., Sadowsky, M.J. (2004). “Arsenic availability from chromated copper arsenate (CCA)-treated wood.” *Journal of environmental quality* **33**: 173–80.

Robert, K. C., and Lipmann, F. (1953) “The effect of arsenate on aerobic phosphorylation”. *Journal of Biological Chemistry*, **201**: 235-243.

Robson, A. O. and Jelliffe, A. M. (1963) “Medicinal Arsenic Poisoning and Lung Cancer”. *British Medical Journal*, **2**: 5351.

Roy, P., and Saha, A. (2002) “Metabolism and toxicity of arsenic: A human carcinogen”. *Current Science*, **82**:38-45.

Russo, M.W., and Murray, S.C. (1997) “Plasma selenium levels and the risk of colorectal adenomas”, *Nutrition and Cancer*, **28**: 125-129.

Ruyle, G. (2009) "Poisonous Plants on Arizona Rangelands". The University of Arizona.<http://cals.arizona.edu/arec/pubs/rmg/1%20rangelandmanagement/2%20poisonousplants93.pdf>

Schafer, F.Q., and Buettner, G.R. (2001) "Redox Environment of the cell as viewed through the redox state of the glutathione disulfide/glutathione couple". *Free Radical Biology & Medicine,* **30**:1191-1212.

Schulze, D.G., and Bertsch, P.M. (1995) "Synchrotron X-ray techniques in soil, plant, and environmental research". *Advances in Agronomy*, **55**:1-66**.**

Sheng, T., (2003) "L. Selenium". *Chemical and Engineering News*, **81**: 94.

Steiner-Asiedu, M., Anderson, A.K., Vuvor, F., and Asiedu, D.K. (2010) "Exposure to Arsenic in Drinking Water-Public Health Debates and Concerns". *Research Journal of Environmental and Earth Sciences*, 2: 1-5.

Styblo, M., Del Razo, L.M., Vega, L., Germolec, D. R., Lecluyse, E.L., Hamilton, G.A., Reed, W., Wang, C. Cullen, W.R., and Thomas, D.J. (2000) "Comparative toxicity of trivalent and pentavalent inorganic and methylated arsenicals in rat and human cells**".** *Achieves of Toxicology*, **74:289**-299.

Teo, B.K. (1986) "EXAFS: basic principles and data analysis". 349-351, Berlin and New York, Springer-Verlag.

Thavarajah, D., Vandenberg, A., George, G. N., and Pickering, I. J. (2007) "The Chemical Form of Selenium in Naturally Selenium-Rich Lentils (*Lens culinaris L.*) from Saskatchewan", *Journal of Agricultural and Food Chemistry*, **55**:7337-7341.

Theil, E. C., Sayers, D. E., and Brown, M. A. (1979) “Similarity of Structure of Ferritin and Iron Dextran (Imferon) Determined by Extended X-ray Absorption Fine Structure Analysis”. *The Journal of Biological Chemistry*, **254**: 8132-8134

Thomas, D. J., Styblo, M., and Lin, S. (2001) “The cellular metabolism and systemic toxicity of arsenic”. *Toxicology and Applied Pharmacol*ogy, **176**: 127–144.

Utiger, R. D. (1998) “Kashin–Beck Disease — Expanding the Spectrum of Iodine-Deficiency Disorders”. *The New England Journal of Medicine,* 339:1156-1158.

Vahter, M. (1994) “Species differences in the metabolism of arsenic compounds”. *Applied Organometallic Chemistry,* **8**: 175-182.

Van Elp, J., Peng, G., Zhou, Z.H., Adams, M.W.W., Baidya, N., Mascharak, P.K., and Cramer, S.P. (1995) “Nickel L-Edge X-ray Absorption Spectroscopy of Pyrococcus furiosus Hydrogenase”. *Inorganic Chemistry,* **34**:2501-2504.

Vendeland, S.C., Butler, J.A., and Whanger, P.D. (1992) “Intestinal absorption of selenite, selenate, and selenomethionine in the rat”. *The Journal of Nutritional Biochemistry*, **3**:359-365.

Vigo, J. B., and Ellzey, J. T. (2006) “Effects of Arsenic Toxicity at the Cellular Level: A Review”. *Texas Journal of Microscopy,* **37**: 45–49.

Villamor, E., Mugusi, F., Urassa, W., Bosch, R.J., Saathoff, E., Matsumoto, K., Meydani, S.N., and Fawzi, W.W. (2008) “A trial of the effect of micronutrient supplementation on treatment outcome, T cell counts, morbidity, and mortality in adults with pulmonary tuberculosis”. *The Journal of Infectious Diseases*, **197**: 1499–505.

Warner, M.L., Moore, L.E., Smith, M.T., Kalman, D.A., Fanning, E., and Smith, A.H. (1994) “Increased micronuclei in exfoliated bladder cells of individuals who chronically ingest arsenic-contaminated water in Nevada”. *Cancer Epidemiology, Biomarkers & Prevention,* **3**: 583–90.

Watanabe, C. (2002) "Modification of mercury toxicity by selenium: practical importance?” *The Tohoku Journal of Experimental Medicine*, **196**: 71–7.

Whanger, P. D. (2002) “Selenocompounds in Plants and Animals and their Biological Significance” *Journal of the American College of Nutrition,* **21**:223–232.

WHO (World Health Organization), (2001) “Arsenic in drinking water”, *Fact sheet N^{o}210,* <http://www.who.int/mediacentre/factsheets/fs210/en/print.html>

Zeng, H., Uthus, E.O., Combs Jr, G.F. (2005) “Mechanistic aspects of the interaction between selenium and arsenic”. *Journal of inorganic chemistry* ,**99**:1269-1274.

Zhang, J.S., Gao, X.Y., Zhang, L.D., and Bao, Y.P. (2001) “Biological effects of a nano red elemental selenium”. *Biofactors*, **15**:27–38.